Table 1. Clinical characteristics of the study population

	men (n=1,917)	women (n=1,347)
age	46.3 ± 0.30	45.7 ± 0.46
BMI	23.4 ± 0.07	22.4 ± 0.07*
waist circumference (cm)	84.1 ± 0.20	73.2 ± 0.29*
systolic blood pressure (mmHg)	125 ± 0.40	120 ± 0.49*
diastolic blood pressure (mmHg)	76.3 ± 0.27	72.3 ± 0.31*
T-cho (mg/dL)	201 ± 0.78	200 ± 0.97
TG (mg/dL)	145 ± 2.97	92.1 ± 1.64*
HDLc (mg/dL)	54.8 ± 0.33	64.6 ± 0.39*
LDLc (mg/dL)	118.0 ± 0.99	113.5 ± 1.22**
HbA1c (%)	4.86 ± 0.02	4.82 ± 0.14
fasting glucose (mg/dL)	97.8 ± 0.43	91.1 ± 0.36*
insulin (IU/mL)	6.28 ± 0.11	7.16 ± 0.21*

Data are expressed as the means ± SEM. T-cho; total cholesterol, TG; triglyceride, HDLc; HDL-cholesterol, LDLc; LDL-cholesterol. *$p<0.001$, **$p<0.01$

emia were excluded, because we could not obtain data as to whether they were treated for hypercholesterolemia or hypertriglyceridemia. We also analyzed the incidence of metabolic syndrome by ATP III criteria published in 2005[9]. We modified the criteria by using the Japanese cutoff of waist circumference. Other differences are fasting glucose ≧100 mg/dL and HDL-cholesterol <50 mg/dL in women. Metabolic syndrome in ATP III criteria was defined as the presence of at least 3 abnormalities among visceral obesity, hypertriglyceridemia, low HDL-cholesterolemia, hypertension, and glucose intolerance.

Data Analysis

The results are expressed as the mean value ± standard deviation, and categorical data by the incidence and relation between visceral obesity and various factors were expressed by the odds ratio and 95% confidence interval. Differences in the means were evaluated by analysis of variance (ANOVA) or analysis of covariance (ANCOVA). The relation between visceral obesity and various factors was examined using multiple, logistic regression analysis for multivariate analysis. Analysis was performed using the statistical Package for Social Sciences (SPSS Japan Inc. ver. 11.5, Tokyo, Japan). A p value of 0.05 or less was considered to indicate significant difference.

Results

Table 1 shows the characteristics of the study population. The means of total cholesterol, triglyceride, HDL-cholesterol, and fasting glucose were 200 mg/dL, 123 mg/dL, 59 mg/dL, and 95 mg/dL. These data are almost the same as the means of the total participants (201, 115, 59, 95, respectively)[6]. The means of both genders were also equivalent to the means of the total participants, indicating that this population represents all participants in this Japanese lipid survey in 2000. Although we found no difference in the mean age, total cholesterol, and HbA1c between men and women, the means of BMI, waist circumference, blood pressure, triglyceride, LDL-cholesterol, and fasting glucose were higher in men than in women, while those of HDL-cholesterol and insulin were lower in men than in women.

Table 2. Incidence of metabolic syndrome and metabolic abnormalities by Japanese diagnostic criteria

	men (%)	women (%)	all (%)
metabolic syndrome	12.1	1.7	7.8
visceral obesity	48.2	9.7	32.3
hypertriglyceridemia	31.3	11.2	23.0
low HDL-cholesterolemia	12.4	2.2	8.2
dyslipidemia	35.2	12.1	25.6
hypertension	25.4	19.5	22.9
elevated fasting glucose	14.4	7.0	11.3

Dyslipidemia is defined as hypertriglyceridemia and/or low HDL-cholesterolemia

Using the Japanese diagnostic criteria for metabolic syndrome we determined the incidence of metabolic syndrome (**Table 2**). The incidence of metabolic syndrome in all participants was 7.8%. The incidence in men and women was 12.1, 1.7%, respectively. The incidence was about 7-fold higher in men than in women, reflecting the difference in visceral obesity defined by waist circumference, 48.2% in men and 9.7% in women. The incidence of dyslipidemia, hypertension, and glucose intolerance was also higher in men than in women in this population, indicating a higher prevalence of metabolic abnormalities in men.

It is important for us to intervene from the period of visceral obesity to prevent cardiovascular disease due to these metabolic abnormalities. Therefore, we compared the incidence of visceral obesity, visceral obesity plus one metabolic abnormality, and metabolic syndrome. **Fig. 1** shows the incidence of visceral obesity, visceral obesity plus one metabolic abnormality, and metabolic syndrome. The incidence of visceral obesity plus one metabolic abnormality was about twice the incidence of metabolic syndrome both in men and women.

To compare the incidence of metabolic syndrome

by Japanese and ATP III criteria in this population, we determined the incidence of metabolic syndrome using these criteria in each generation from age 20s to 70s in men and women as shown in **Fig. 2**. The incidence of metabolic syndrome using ATP III criteria was about 3 times higher than that by the Japanese criteria. Using both criteria the incidence of metabolic syndrome started to rise in men in their 30s and reached a plateau after their 40s. Meanwhile, the incidence of metabolic syndrome in women started to rise after their 50s using both criteria, indicating the increased prevalence of metabolic syndrome after menopause.

We next examined whether visceral obesity contributed to metabolic abnormalities in this study population. **Fig. 3** shows the difference of lipid profiles and fasting glucose levels with or without visceral obe-

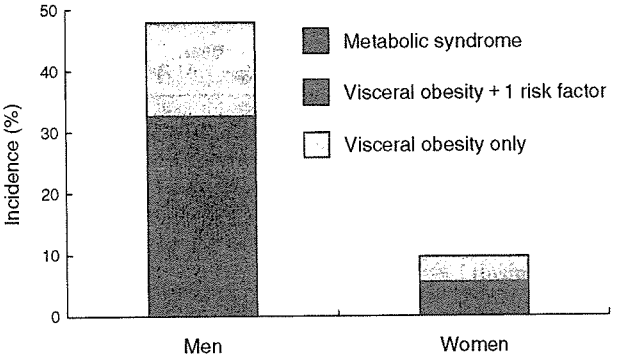

Fig. 1. Incidence of metabolic syndrome and visceral obesity in the lipid survey in 2000.

The percent incidence of metabolic syndrome, visceral obesity plus one risk factor, and visceral obesity in men and women is shown.

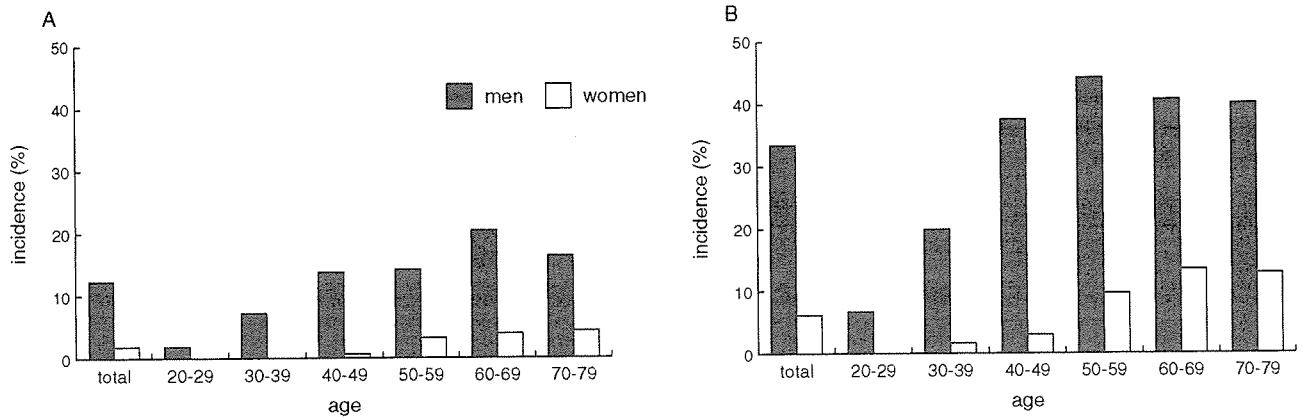

Fig. 2. Incidence of metabolic syndrome in each generation by Japanese and ATP III criteria.

Each column shows the incidence of metabolic syndrome in each generation in men (closed column) and women (open column) by Japanese (A) and ATP III (B) criteria. The incidence in the total population is shown on the left.

Fig. 3. Comparison of metabolic abnormalities with or without visceral obesity.

Each column shows the mean ± SD of total cholesterol, triglyceride, HDL-cholesterol, LDL-cholesterol, and fasting glucose with or without visceral obesity in men (A) and women (B). $*p < 0.001$

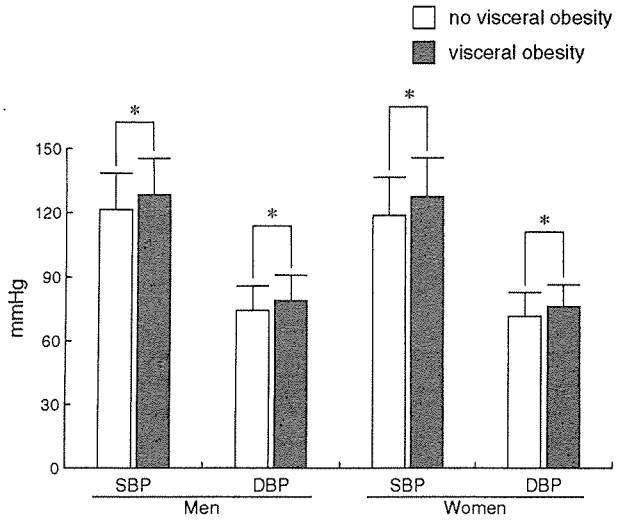

Fig. 4. Comparison of systolic and diastolic pressure with or without visceral obesity.

Each column shows the mean ± SD of systolic and diastolic blood pressure with or without visceral obesity in men and women. $^{*}p < 0.001$

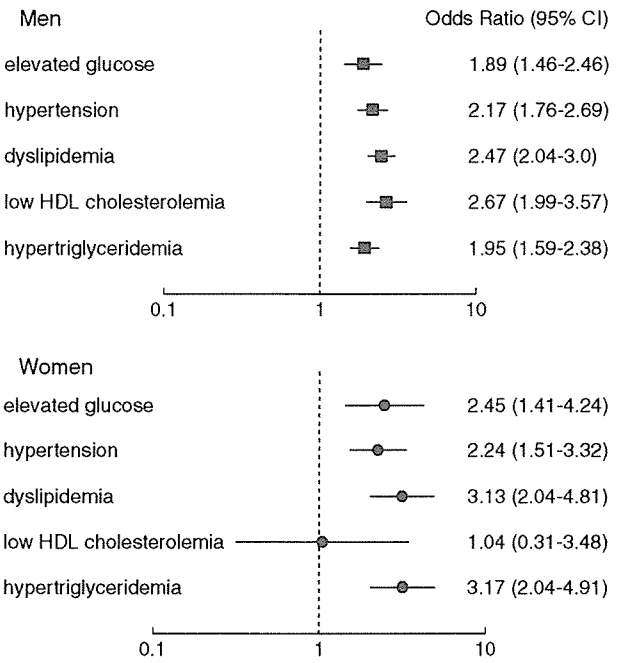

Fig. 5. Effect of visceral obesity on hypertriglyceridemia, low HDL cholesterolemia, dyslipidemia, hypertension, and glucose intolerance in men and women.

Odds ratios and 95% confidence interval are shown for each abnormality in the presence or absence of visceral obesity.

sity in this study population. The levels of total cholesterol, triglyceride, LDL-cholesterol, and fasting glucose were significantly higher, while the level of HDL-cholesterol was significantly lower in the group with visceral obesity than in the group without, indicating the contribution of visceral obesity to these metabolic abnormalities in both men and women. Systolic and diastolic blood pressure was also higher in the visceral obesity group in both genders (**Fig. 4**). We also determined the effect of visceral obesity on the development of each abnormality by calculating the odds ratios and 95% confidence interval (**Fig. 5**). Visceral obesity was significantly associated with the development of each metabolic abnormality in men and women except for low HDL-cholesterolemia in women. When we changed the cutoff of HDL-cholesterol to 50 mg/dL, visceral obesity was significantly associated with low HDL-cholesterolemia in women. The odds ratio was 2.10 and the 95% confidence interval was 1.35-3.27. Among dyslipidemia, hypertension, and glucose intolerance, visceral obesity was most associated with the development of dyslipidemia.

We also determined the age-adjusted difference of lipid profile in the presence or absence of visceral obesity in this population. Even after age adjustment we found a significant difference in total cholesterol, triglyceride, HDL-cholesterol, and LDL-cholesterol in men and in women, except for a difference in LDL-cholesterol in women (**Table 4**).

Discussion

In this study we determined the incidence of metabolic syndrome in the Japanese general population using a lipid survey performed in 2000 using new Japanese criteria to diagnose metabolic syndrome. We found that 3 times more people were diagnosed with metabolic syndrome using the new ATP III criteria than the Japanese criteria and that visceral obesity contributed to metabolic abnormalities, such as dyslipidemia, glucose intolerance, and hypertension.

In our study the incidence of metabolic syndrome in Japanese men and women was 12.1 and 1.7%, respectively. The incidence of metabolic syndrome in our survey is lower than that from the latest National Health and Nutrition survey in 2004. In that survey the incidence of metabolic syndrome in Japanese men and women was 23.0 and 8.9%, respectively. In this national survey they used HbA1c ($\geqq$5.5) instead of FBS to diagnose glucose intolerance. This might explain the difference between the two surveys. This difference also indicates that the cutoff of FBS needs to be changed in the future. Although the mean age and the criteria used were different, Takeuchi *et al.*

Table 3. Incidence of each metabolic abnormality in the presence or absence of visceral obesity

	visceral obesity		no visceral obesity	
	men	women	men	women
hypertriglyceridemia	41.1%	25.4%	22.2%	9.7%
low HDL-cholesterolemia	17.6%	2.3%	7.4%	2.2%
dyslipidemia	45.7%	26.9%	25.4%	10.5%
hypertension	32.8%	33.1%	18.4%	18.1%
elevated fasting glucose	18.4%	14.6%	10.6%	6.2%

Dyslipidemia is defined as hypertriglyceridemia and/or low HDL-cholesterolemia

Table 4. Age-adjusted difference of lipid profile in the presence or absence of visceral obesity

		men		age-adjusted	women		age-adjusted	all		age-adjusted
		no visceral obesity	visceral obesity	*P*	no visceral obesity	visceral obesity	*P*	no visceral obesity	visceral obesity	*P*
T-cho	mean	195.6	205.9		198.8	214.2		197.3	206.9	
	number	994	923	<0.001	1217	130	0.082	2211	1053	<0.001
	SD	33.4	33.4		35.4	33.1		34.6	33.4	
TG	mean	128.7	162.0		88.9	121.7		106.8	157.0	
	number	994	923	<0.001	1217	130	<0.001	2211	1053	<0.001
	SD	119.3	138.8		60.2	51.5		93.7	131.8	
HDLc	mean	57.7	51.7		65.1	59.8		61.8	52.7	
	number	994	923	<0.001	1217	130	0.003	2211	1053	<0.001
	SD	14.2	13.9		14.5	12.5		14.8	14.0	
LDLc	mean	112.1	122.1		111.4	128.0		111.7	122.9	
	number	374	479	0.001	510	71	0.106	884	550	<0.001
	SD	26.0	30.1		29.0	28.8		27.8	30.0	

The mean, the number of samples, and SD are shown. *P* value was obtained by ANCOVA.

reported that the incidence of metabolic syndrome in men in the Tanno and Sobetsu study was 25.3%[11]. The mean age of their study population was 60.3 years, about 15 years older than that in our study population. Other studies reported a similar incidence of metabolic syndrome in Japanese. Considering that the incidence of metabolic syndrome in our population in their 60s was about 20%, the difference of the criteria used contributed to this difference. Similar to our study Urashima *et al.* reported an incidence of metabolic syndrome in Japanese men and women of 14.1% and 1.7%, respectively in central Tokyo[12]. Thus, the current incidence of metabolic syndrome in Japan would be around 15% in men and a few percent in women. In our study we found that about twice as many people with metabolic syndrome had visceral obesity and one risk factor in both men and women, indicating a potential for the incidence of metabolic syndrome to increase in the future. In our previous analysis we showed that the level of triglyceride in men dramatically increased from 1990 to 2000[6]. Therefore, we need to tackle this problem to prevent the increase in metabolic syndrome and cardiovascular disease in Japan.

In this population the incidence of metabolic syndrome in women was one seventh that in men. The incidence of visceral obesity, dyslipidemia, and glucose intolerance in women was one fifth, one third, and one half that in men, respectively. Furthermore, most of the women who satisfied this criteria were more than 50 years old, which means that few women are diagnosed with metabolic syndrome before the menopause. In Japan we adopted a cutoff of waist circumference of 90 cm for women, which is 5 cm more than that for men. This might explain why the incidence of metabolic syndrome in women was much less than in men. In contrast to the cutoff waist circumference in Japan, other criteria, such as in ATP Ⅲ,

generally have a larger cutoff in men than in women; however, our cutoff in women is based on the extensive study by Matsuzawa and his group using CT scan[13-15]. Therefore, in terms of detecting visceral obesity, 90 cm would be appropriate for Japanese women. However, we need to establish another method to select high-risk patients without visceral obesity. Our data also strongly indicate that visceral obesity using our cutoff is associated with metabolic abnormalities even after age adjustment, as shown in **Fig. 5** and **Table 4**. Therefore, we believe that visceral obesity is a useful surrogate marker for metabolic abnormalities and intervention to reduce abdominal circumference would lead to the prevention of cardiovascular disease. However, in terms of the cutoff of HDL-cholesterol, 50 mg/dL might be better than 40 mg/dL from the odds ratio in women (**Fig. 5** and Results) as in the cutoff of the ATP III criteria.

In summary we have shown that the incidence of metabolic syndrome in the Japanese general population is 7.8%, 12.1% in men and 1.7% in women. Intervention is required to prevent metabolic syndrome as well as metabolic abnormalities, such as dyslipidemia, hypertension, and glucose intolerance. The current criteria for metabolic syndrome should be assessed for the better diagnosis of women and elderly people.

Acknowledgements

This study was supported by research grants for health sciences from the Japanese Ministry of Health and a grant from the Japan Atherosclerosis Society. We thank Shizuya Yamashita (Osaka University) and Hideaki Bujo (Chiba University) for critical reading of the manuscript. We also thank Osaka Pharmaceutical Manufacturers Association for supporting our work.

References

1) Third Report of the National Cholesterol Education Program (NCEP) Expert Panel on Detection, Evaluation, and Treatment of High Blood Cholesterol in Adults (Adult Treatment Panel III) final report. Circulation, 2002; 106:3143-3421.
2) Matsuzawa Y: Therapy Insight: adipocytokines in metabolic syndrome and related cardiovascular disease. Nat Clin Pract Cardiovasc Med, 2006; 3:35-42
3) Lemieux I, Pascot A, Couillard C, Lamarche B, Tchernof A, Almeras N, Bergeron J, Gaudet D, Tremblay G, Prud'homme D, Nadeau A, and Despres JP: Hypertriglyceridemic waist: A marker of the atherogenic metabolic triad (hyperinsulinemia; hyperapolipoprotein B; small, dense LDL) in men? Circulation, 2000; 102:179-184.
4) Carr DB, Utzschneider KM, Hull RL, Kodama K, Retzlaff BM, Brunzell JD, Shofer JB, Fish BE, Knopp RH, and Kahn SE: Intra-abdominal fat is a major determinant of the National Cholesterol Education Program Adult Treatment Panel III criteria for the metabolic syndrome. Diabetes, 2004; 53:2087-2094.
5) Ford ES, Giles WH, and Dietz WH: Prevalence of the metabolic syndrome among US adults: findings from the third National Health and Nutrition Examination Survey. JAMA, 2002; 287:356-359.
6) Arai H, Yamamoto A, Matsuzawa Y, Saito Y, Yamada N, Oikawa S, Mabuchi H, Teramoto T, Sasaki J, Nakaya N, Itakura H, Ishikawa Y, Ouchi Y, Horibe H, and Kita T: Serum lipid survey and its recent trend in the general Japanese population in 2000. J Atheroscler Thromb, 2005; 12:98-106.
7) Yamamoto A, Horibe H, Mabuchi H, Kita T, Matsuzawa Y, Saito Y, Nakaya N, Fujioka T, Tenba H, Kawaguchi A, Nakamura H, and Goto Y: Analysis of serum lipid levels in Japanese men and women according to body mass index. Increase in risk of atherosclerosis in postmenopausal women. Research Group on Serum Lipid Survey 1990 in Japan. Atherosclerosis, 1999; 143:55-73.
8) Matsuzawa Y: Metabolic syndrome--definition and diagnostic criteria in Japan. J Atheroscler Thromb, 2005; 12:301.
9) Grundy SM, Cleeman JI, Daniels SR, Donato KA, Eckel RH, Franklin BA, Gordon DJ, Krauss RM, Savage PJ, Smith SC Jr., Spertus JA, and Costa F: Diagnosis and management of the metabolic syndrome: an American Heart Association/National Heart, Lung, and Blood Institute Scientific Statement. Circulation, 2005; 112:2735-2752.
10) Johnson CL, Rifkind BM, Sempos CT, Carroll MD, Bachorik PS, Briefel RR, Gordon DJ, Burt VL, Brown CD, Lippel K, et al.: Declining serum total cholesterol levels among US adults. The National Health and Nutrition Examination Surveys. JAMA, 1993; 269:3002-3008.
11) Takeuchi H, Saitoh S, Takagi S, Ohnishi H, Ohhata J, Isobe T, and Shimamoto K: Metabolic syndrome and cardiac disease in Japanese men: applicability of the concept of metabolic syndrome defined by the National Cholesterol Education Program-Adult Treatment Panel III to Japanese men--the Tanno and Sobetsu Study. Hypertens Res, 2005; 28:203-208.
12) Urashima M, Wada T, Fukumoto T, Joki M, Maeda T, Hashimoto H, and Oda S: Prevalence of metabolic syndrome in a 22,892 Japanese population and its associations with life style. JMAJ, 2005; 48:441-450.
13) Matsuzawa Y, Shimomura I, Nakamura T, Keno Y, and Tokunaga K: Pathophysiology and pathogenesis of visceral fat obesity. Diabetes Res Clin Pract, 1994; 24 Suppl: S111-116.
14) Tokunaga K, Matsuzawa Y, Ishikawa K, and Tarui S: A novel technique for the determination of body fat by computed tomography. Int J Obes, 1983; 7:437-445.
15) Yoshizumi T, Nakamura T, Yamane M, Islam AH, Menju M, Yamasaki K, Arai T, Kotani K, Funahashi T, Yamashita S, and Matsuzawa Y: Abdominal fat: standardized technique for measurement at CT. Radiology, 1999; 211:283-286.

roiditis in patients with polycystic ovary syndrome. Eur J Endocrinol 2004;150:363–9.
4. Glintborg D, Hermann AP, Brusgaard K, Hangaard J, Hagen C, Andersen M. Significantly higher adrenocorticotropin-stimulated cortisol and 17-hydroxyprogesterone levels in 337 consecutive, premenopausal, Caucasian, hirsute patients compared with healthy controls. J Clin Endocrinol Metab 2005;90:1347–53.

Anargyros Kourtis*
David Rousso
Christos Balaris
Dimitrios Farmakiotis
Ilias Katsikis
Dimitrios Panidis

Division of Endocrinology and Human Reproduction
Second Department of Obstetrics and Gynecology
Aristotle University of Thessaloniki
Thessaloniki, Greece

* Address correspondence to this author at: Division of Endocrinology and Human Reproduction, Second Department of Obstetrics and Gynecology, Aristotle University of Thessaloniki, 49 Konstantinoupoleos, 54642 Thessaloniki, Greece.

DOI: 10.1373/clinchem.2006.071076

ELISA for Soluble Form of Lectin-Like Oxidized LDL Receptor-1, A Novel Marker of Acute Coronary Syndrome

To the Editor:

Lectin-like oxidized LDL receptor-1 (LOX-1) is prominently expressed in atherosclerotic plaques *(1, 2)*. LOX-1 expressed on the cell surface is proteolytically cleaved at its membrane-proximal extracellular domain (ECD) and released in soluble form (sLOX-1) *(2, 3)*. Serum sLOX-1 is increased at an earlier stage of acute coronary syndrome (ACS) than are other cardiac makers, such as creatine kinase-MB fraction, troponin T, and high-sensitivity C-reactive protein *(4)*. We describe the development of an ELISA for sLOX-1.

The cleavage sites on human LOX-1 (hLOX-1) remain unknown. We tried to obtain human sLOX-1 (hsLOX-1) from cultures of CHO-K1 cells stably expressing hLOX-1 *(3, 5)*, but the amount of hsLOX-1 obtained was too small for ELISA development.

hsLOX-1 should be similar to the ECD of hLOX-1 (hLOX-1-ECD), considering a structure of bovine sLOX-1 *(3)*. We produced recombinant hLOX-1-ECD [rhLOX-1-ECD; hLOX-1 (84–273)] in *Escherichia coli* and purified it as described previously *(5)*; we then used the soluble fraction of rhLOX-1-ECD instead of hsLOX-1 as the assay calibrator and immunogen. We estimated the amount of rhLOX-1-ECD by ultraviolet spectrophotometry, using the formula: $E^{1\%}_{280\ nm} = 10.0$.

To produce the K266 and K267 antisera, we immunized 2 female rabbits (KBL:JW; Kitayama Labs) with an emulsion of rhLOX-1-ECD solution in Freund's complete adjuvant [~0.4 mg (0.5 mL) per dose]. Each rabbit received a dose once every 3 weeks for a total of 6 doses.

We used K266 IgG as the immobilized (capture) antibody and horseradish peroxidase (HRP)-labeled K267 Fab' as the detection antibody. K267 Fab' was prepared and labeled with HRP by use of succinimidyl 4-(*N*-maleimidomethyl)cyclohexane 1-carboxylate (Pierce), as described previously *(6)*. Absorbance ratios at 280 and 403 nm indicated a 1:1 molecular binding ratio of HRP to K267 Fab'. We added the preservative Proclin 150 (final concentration, 1 mL/L; Supelco) to the HRP-labeled antibody, which was stored at −80 °C.

To immobilize the K266 antibody, we added 100 μL of K266 IgG solution (0.01 g/L in 0.1 mol/L phosphate buffer, pH 7.0) to the wells of microplates. The microplates were kept at room temperature for 16 h and then washed twice with 200 μL of assay buffer [0.1 mol/L phosphate buffer (pH 7.0) containing 5 g/L bovine serum albumin (Sigma), 1 g/L CHAPS (Dojindo), and Proclin 150]. The plate was then blocked with the assay buffer (200 μL) for 2 h at room temperature.

Calibrator samples (1–100 μg/L rhLOX-1-ECD in commercially available normal human plasma; George King Biomedical) or unknown samples of human serum/plasma (10 μL) were added to 100 μL of assay buffer in duplicate microplate wells containing immobilized antibody. The microplates were then incubated for 2 h at room temperature and washed twice. The HRP-labeled antibody solution (100 μL; diluted to ~900 μg/L in the assay buffer) was then added to the microplate wells and incubated for 16 h at room temperature. We then washed the microplate wells twice and added the substrate solution (100 μL) containing 3,3′,5,5′-tetramethylbenzidine (TMB+; Dako). We allowed the enzyme reaction to take place for 30 min in the dark and then stopped the reaction with 0.5 mol/L sulfuric acid (100 μL). The absorbance at 450 nm was measured by a plate reader (ARVOsx; Wallac/Perkin-Elmer).

We evaluated the effects of endogenous sLOX-1 by assaying 10-μL samples of individual plasmas from 6 healthy volunteers and the commercially available plasma; the differences between the results were negligible. ELISA binding was not changed in plasma samples containing heparin, EDTA, or citrate, and we observed no differences between plasma and serum. Various substances (final concentrations: bilirubin F, 34–170 mg/L; bilirubin C, 42–210 mg/L; hemolytic hemoglobin, 1–5 g/L; chyle, 392-1960 FTU; Interference check-A; International Reagent Corp.) in the calibrator samples (50 μg/L) did not interfere with the ELISA. The presence of oxidized or native LDL (3.2–50 000 μg/L), which may bind sLOX-1 in the calibrator solutions (10 μg/L), had no effect *(4)*.

The ELISA calibration curve indicated a good response to rhLOX-1-ECD (1–100 μg/L) as well as to hsLOX-1 (Fig. 1), suggesting that this ELISA can measure natural forms of human sLOX-1. Intra-/interassay imprecision (as CV) was 2.0%–12%, and measured values were within −2.5% to +7.0% of the expected values for the range 1–100 μg/L. The limit of quantification was 1.0 μg/L. Plasma (serum) concentrations >0.5 μg/L were detectable; however, de-

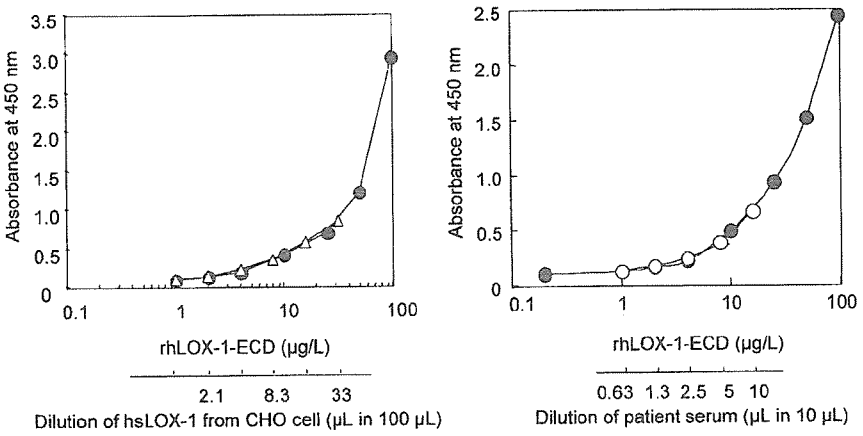

Fig. 1. ELISA calibration curves.

(*Left*), ELISA calibration curve for rhLOX-1-ECD in the assay buffer (●) and comparison with the dilution curve for sLOX-1 obtained from the conditioned media of hLOX-1-CHO cells (△). Although hsLOX-1 released from hLOX-1-CHO cells was not used as the assay calibrator, its response in the ELISA at various dilutions matched the ELISA calibration curve obtained by use of rhLOX-1-ECD. (*Right*), calibration curve for rhLOX-1-ECD in normal human plasma (●) and comparison with the dilution curve for a patient serum sample with a high sLOX-1 concentration (○). The responses of serial dilutions of patient serum were comparable to the ELISA calibration curve, thus demonstrating that this ELISA measures sLOX-1 in human blood.

tection of concentrations <1 μg/L was unreliable.

rhLOX-1-ECD in plasma at concentrations of 1.79, 8.64, and 41.4 μg/L was stable at −40 °C for 14 weeks and during 3 freeze–thaw cycles.

Our results indicate that the proposed ELISA measured sLOX-1 specifically and sensitively in human serum/plasma and can be used as a diagnostic test for ACS at the earliest stage.

References

1. Kataoka H, Kume N, Miyamoto S, Minami M, Moriwaki H, Sawamura T, et al. Expression of lectin-like oxidized low density lipoprotein receptor-1 in human atherosclerotic lesions. Circulation 1999;99:3110–7.
2. Kume N, Kita T. Roles of lectin-like oxidized low density lipoprotein receptor-1 (LOX-1) and its soluble forms in atherogenesis. Curr Opin Lipidol 2001;12:419–23.
3. Murase T, Kume N, Kataoka H, Minami M, Sawamura T, Masaki T, Kita T. Identification of soluble forms of lectin-like oxidized LDL receptor-1. Arterioscler Thromb Vasc Biol 2000;20:715–20.
4. Hayashida K, Kume N, Murase T, Minami M, Nakagawa D, Inada T, et al. Serum soluble lectin-like oxidized low-density lipoprotein receptor-1 levels are elevated in acute coronary syndrome: a novel marker for early diagnosis. Circulation 2005;112:812–8.
5. Hayashida K, Kume N, Minami M, Kita T. Lectin-like oxidized LDL receptor-1 (LOX-1) supports adhesion of mononuclear leukocytes and a monocytes-like cell line THP-1 cells under static and flow conditions. FEBS Letters 2002;511:133–8.
6. Ishikawa E, Imagawa M, Hashida S, Yoshitake S, Hamaguchi Y, Ueno T. Enzyme-labeling of antibodies and their fragments for enzyme immunoassay and immunohistochemical staining. J Immunoassay 1983;4:209–327.

Akira Ueda[1]
Noriaki Kume[2]
Kazutaka Hayashida[2]
Atsuko Inui-Hayashida[2]
Mika Asai[1]
Toru Kita[2]
Goro Kominami[1]*

[1] *Shionogi Research Laboratories*
Shionogi & Co. Ltd.
Osaka, Japan

[2] *Department of*
Cardiovascular Medicine
Graduate School of Medicine
Kyoto University
Shogoin, Sakyo-ku
Kyoto, Japan

* Address correspondence to this author at: Shionogi Research Laboratories, Shionogi & Co. Ltd., 5-12-4 Sagisu, Fukushima-ku, Osaka 553-0002, Japan. Fax 81-6-6458-0987; e-mail goro.kominami@shionogi.co.jp.

DOI: 10.1373/clinchem.2005.064808

N-Terminal Pro-B-Type Natriuretic Peptide and Echocardiographic Abnormalities in Severely Obese Patients: Correlation with Visceral Fat

To the Editor:

B-Type natriuretic peptide (BNP) and its co-released peptide N-terminal propeptide (NT-proBNP) are both secreted mainly by the left cardiac ventricle as a consequence of pressure overload and wall stretch. This situation often occurs in obesity, in which the amount of intraabdominal fat may worsen the severity of morphologic and dynamic cardiac abnormalities detectable by echocardiography (*1*).

Many studies have confirmed NT-proBNP as a sensitive marker for left ventricular hypertrophy and/or asymptomatic left ventricular dysfunction (*2*, *3*), and it is particularly reliable because of its high negative predictive value (*4*). To our knowledge, however, recent findings on the relationship between NT-proBNP and morphologic and dynamic cardiac abnormalities in obesity are still inconsistent and controversial. Rivera et al. (*5*) reported lower NT-proBNP concentrations in obese patients with heart failure compared with nonobese patients. Conversely, Hermann-Arnhof et al. (*6*) found that NT-proBNP concentrations were increased in obese individuals and were comparable to the values for New York Heart Association class I patients. Therefore, to gain further information on the utility of NT-proBNP as an indicator of possible preclinical cardiac disease in normotensive, severely obese individuals, we measured NT-proBNP concentrations in 27 severely obese women with no complications [mean (SD) body mass index, 43.5 (4.8) kg/m^2 (median, 41.7 kg/m^2); mean (SD) age, 33.3 (8.3) years (median, 31 years)] and 15 normal-weight patients. All participants were premenopausal, normotensive, normoglycemic, drug-free young women with normal renal function, who were not dyspneic; this excluded the possibility that high NT-proBNP

Available online at www.sciencedirect.com
SCIENCE DIRECT®
Biochemical and Biophysical Research Communications 341 (2006) 591–598
BBRC
www.elsevier.com/locate/ybbrc

Expression of lectin-like oxidized LDL receptor-1 in smooth muscle cells after vascular injury

Hideyuki Eto [a], Masaaki Miyata [a,*], Noriaki Kume [b], Manabu Minami [b], Hiroyuki Itabe [c], Koji Orihara [a], Shuichi Hamasaki [a], Sadatoshi Biro [a], Yutaka Otsuji [a], Toru Kita [b], Chuwa Tei [a]

[a] *Department of Cardiovascular, Respiratory and Metabolic Medicine, Graduate School of Medicine, Kagoshima University, 8-35-1 Sakuragaoka, Kagoshima 890-8520, Japan*
[b] *Department of Cardiovascular Medicine, Graduate School of Medicine, Kyoto University, 54 Kawahara-cho, Shogoin, Sakyo-ku, Kyoto 606-8507, Japan*
[c] *Department of Biological Chemistry, School of Pharmaceutical Sciences, Showa University, 1-5-8 Hatanodai, Shinagawa-ku, Tokyo 142-8555, Japan*

Received 18 December 2005
Available online 13 January 2006

Abstract

Lectin-like oxidized LDL receptor-1 (LOX-1) is an oxidized LDL receptor, and its role in restenosis after angioplasty remains unknown. We used a balloon-injury model of rabbit aorta, and reverse transcription-polymerase chain reaction revealed that LOX-1 mRNA expression was modest in the non-injured aorta, reached a peak level 2 days after injury, and remained elevated until 24 weeks after injury. Immunohistochemistry and in situ hybridization showed that LOX-1 was not detected in the media of non-injured aorta but expressed in both medial and neointimal smooth muscle cells (SMC) at 2 and 24 weeks after injury. Low concentrations of ox-LDL (10 μg/mL) stimulated the cultured SMC proliferation, which was inhibited by antisense oligonucleotides of LOX-1 mRNA. Double immunofluorescense staining showed the colocalization of LOX-1 and proliferating cell nuclear antigen in human restenotic lesion. These results suggest that LOX-1 mediates ox-LDL-induced SMC proliferation and plays a role in neointimal formation after vascular injury.

Keywords: LOX-1; Angioplasty; Restenosis; Vascular smooth muscle cell

Oxidized low-density lipoprotein (ox-LDL) is believed to play a key role in cellular dysfunction, as well as cholesterol accumulation and subsequent foam-cell transformation in macrophages and phenotypically modulated vascular smooth muscle cells (SMC) [1]. Lectin-like oxidized LDL receptor-1 (LOX-1), a new class of oxidized LDL receptors, is expressed by intimal SMC and macrophages in advanced atherosclerotic lesions, as well as vascular endothelial cells covering early atherosclerotic lesions [2,3]. Therefore, LOX-1 is thought to play a role in the atherogenesis and the pathogenesis of atherosclerotic plaque rupture [4] and inflammatory intramyocardial vasculopathy [5].

Percutanous coronary intervention (PCI) is an important procedure for the treatment of coronary stenosis. Sirolimus-eluting and polymeric paclitaxel-eluting stents strongly suppress neointimal hyperplasia [6,7]. However, a meta-analysis of randomized clinical trials of drug-eluting stents reported that the rate of angiographic restenosis after drug-eluting stents is 8.9% [8]. Restenosis after PCI is still a significant problem. Identifying the molecules involved in the restenosis after PCI will help to develop new strategies for the prevention of restenosis.

Although roles of LOX-1 in atherosclerotic plaque stability have been suggested [4], its role in restenosis after PCI remains unknown. Therefore, we investigated LOX-1 expression in the neointima and media of the rabbit aorta

* Corresponding author. Fax: +81 99 265 8447.
E-mail address: miyatam@m3.kufm.kagoshima-u.ac.jp (M. Miyata).

0006-291X/$ - see front matter © 2006 Elsevier Inc. All rights reserved.
doi:10.1016/j.bbrc.2005.12.211

after balloon injury, as well as human lesions after PCI. Furthermore, in order to address the role of LOX-1 in neointimal hyperplasia after balloon injury, we performed cell culture experiments.

Methods

Rabbit aorta model. Male Japanese white rabbits weighing 3.0–3.5 kg were used and all surgical procedures on rabbits were carried out under general anesthesia with sodium pentobarbital (40 mg/kg), ketamine (2 mg/kg), and xylazine (8 mg/kg). The balloon-injury model of the rabbit aorta was created as reported previously [9]. At various time points (6, 12, and 24 h, 2, 5, and 7 days, and 2, 4, 8, 16, and 24 weeks after balloon injury), animals were anesthetized with sodium pentobarbital (40 mg/kg), ketamine (2 mg/kg), and xylazine (8 mg/kg), sacrificed with overdose sodium pentobarbital, and the aorta was carefully removed. For immunohistochemical study, three portions of the injured aorta were fixed with 10% neutral buffered formalin for 24 h and then embedded in paraffin. The specimens were cut into 10-μm thick sections and fixed to glass slides. For isolation of RNA and protein, the adventitia was stripped away from the aorta in PBS with the use of fine forceps and then snap-frozen in liquid nitrogen. Sham-operated animals were used as controls. The investigation conforms to Guide for the Care and Use of Laboratory Animals published by the U.S. National Institutes of Health (NIH Publication No. 85-23, revised 1996) and with the principles outlined in the Declaration of Helsinki. This study was carried out in accordance with the Guide for Animal Experimentation, Faculty of Medicine, Kagoshima University.

Immunohistochemical staining. Immunohistochemical staining was performed as described previously [10]. After deparaffinization and hydration of specimens, endogenous peroxidase activity was blocked and the specimen was fixed by immersion in 0.3% H_2O_2 in methanol for 20 min. Immunohistochemistry was performed using a mouse monoclonal antibody against rabbit LOX-1, a mouse monoclonal antibody against rat muscle actin (HHF-35, Enzo Diagnostics), and a mouse monoclonal antibody against human ox-LDL (donated by Dr. Itabe, Showa University, Tokyo, Japan), by use of the labeled streptavidin–biotin complex method (Histofine SAB-PO kit, Nichirei). An anti-rabbit LOX-1 monoclonal antibody was produced by immunizing mice with a recombinant rabbit LOX-1 extracellular domain and subsequent screening of the hybridomas. Immunoreactivity was confirmed by immunostaining of cells transfected with full-length rabbit LOX-1 cDNA. After blocking with 10% rabbit serum, slides were incubated overnight with a primary antibody at 4 °C in a moisture chamber. Slides were washed with Tris-buffered saline (TBS) and incubated with a biotinylated secondary antibody at room temperature for 30 min. After washing with TBS, slides were incubated with streptavidin at room temperature for 30 min and visualized with 3,3′-diaminobenzidine. The specificity of the immunoreaction was evaluated in comparison with negative control specimens in which irrelevant mouse IgG was used instead of primary antibody.

Preparation of protein extracts. Proteins were extracted for Western blot analysis as reported previously [11]. Briefly, rabbit aorta was ground to a fine powder under liquid nitrogen and incubated in ice-cold 0.1% Triton lysis solution [mmol/L: Hepes 10 (pH 7.4), sodium pyrophosphate 50, NaF 50, EDTA 5, EGTA 5, and NaCl 50; and 100 mmol/L Na_3VO_4, 0.1% Triton X-100, 500 mmol/L PMSF, and 10 mg/mL leupeptin] for 30 min. Insoluble matter was removed by centrifugation, and the protein concentration was measured by a bicinchoninic acid assay (Pierce).

Western blot analysis. Western blotting was performed with a NuPAGE Electrophoresis System (Novex) as reported previously [9]. Briefly, 10-μg protein samples were resuspended in reduced sample buffer and then electrophoresed on a 4–12% Bis-Tris gel (Novex) with Mops running buffer; blotted to nitrocellulose; and sequentially probed with polyclonal goat antisera raised against human LOX-1 (Santa Cruz Biotechnology). Horseradish peroxidase-conjugated rabbit anti-goat antibody (Santa Cruz Biotechnology) was then added, and secondary antibody was detected by autoradiography using enhanced chemiluminescence (ECL Plus, Amersham).

Reverse transcription-polymerase chain reaction (RT-PCR) for LOX-1 mRNA. Frozen rabbit aortas were ground to a fine powder under liquid nitrogen, and total RNA was isolated by the guanidium thiocyanate method. For the synthesis of cDNA, 1 μg of total RNA was reverse-transcribed with random hexamers using Super Script II (Gibco-BRL, Life Technologies). The transcribed cDNA was amplified by PCR with specific primers for rabbit LOX-1 and glyceraldehyde-3-phosphate dehydrogenase (GAPDH). Two specific primer pairs corresponding to published sequences were used to amplify LOX-1 (5′-TATGCACA GGTGCTGAAGG-3′ and 5′-CAAGAGGCTCTGAAGAGAATGG-3′) [3], and GAPDH (5′-CAGGAATTCGGTGAAGGTCGGAGTCAAG GG-3′ and 5′-AGTGGATCCGGTCATGAGTCCTCCCAGGAT-3′). The PCR amplification included 35 cycles of denaturing, annealing, and elongation with Ex *Taq* polymerase (Takara Shuzo). Equal amounts of PCR product were subjected to electrophoresis through 1.5% agarose gels and visualized with ethidium bromide. Densitometric analysis was performed to quantify the PCR products using NIH Image software. GAPDH expression was used as a reference for quantification of LOX-1 mRNA.

In situ hybridization for LOX-1 mRNA. In situ hybridization was carried out with thymine–thymine (T–T) dimerized synthetic oligonucleotides complementary to a rabbit LOX-1 mRNA as a probe as reported previously [9]. A 45-base sequence (italic type) complementary to rabbit LOX-1 mRNA was chosen. A computer-assisted search (GenBank) of antisense sequences, as well as the sense sequences, revealed no significant homology with any known sequences other than that of LOX-1. For the haptenization of oligo-DNAs with T–T dimers, 2 or 3 TTA repeats were added to the 5′- and 3′-ends of the native sequences as follows: antisense probe, 5′-TTATTA*CAAGAGGCTCTGAAGAGAATGGACAACTTTTC AGGTCCTTGTCCC*ATTATTATT-3′; sense probe, 5′-TTATTA*GTTCT CCGAGACTTCTCTTACCTGTTGAAAAGTCCAGGAACAGGG*ATTA TTATT-3′.

Cell culture. Rabbit SMC were isolated from the media of rabbit aorta and were cultured as previously described [9]. We confirmed that these cells were 100% positive for smooth muscle α-actin expression. Seventh passage of SMC was seeded into 48-well microplates and incubated with Medium 199 (M199; Gibco-BRL, Life Technologies) containing 10% fetal bovine serum (FBS). To make the cell growth arresting quiescent, they were incubated with M199 containing 0.1% FBS for 24 h.

Antisense phosphorothioate oligonucleotides and sense phosphorothioate oligonucleotides directed to 5′-coding sequence of the human LOX-1 mRNA were designed and manufactured by Sigma Genosys. The antisense oligonucleotides (antisense LOX-1) were synthesized at 16-mer targeted at 5′-CAGTTAAATGAGGCCG-3′part of the LOX-1 cDNA sequence. The sense oligonucleotides (sense LOX-1) were 16-mer targeted at 5′-ACCTACGTGACTACGT-3′ [12,13]. In order to examine effects of ox-LDL–LOX-1 interactions on SMC proliferation, SMC were preincubated with antisense LOX-1 or sense LOX-1 (0.5 μmol/L) containing 0.1% FBS for 48 h and then incubated with ox-LDL (10 μg/mL) containing 0.1% FBS for 24 h. We counted the cell numbers to determine the SMC proliferation. To analyze the expression of LOX-1 and proliferating cell nuclear antigen (PCNA), SMC were cultivated on chamber slides in the presence of antisense or sense LOX-1 (0.5 μmol/L) for 48 h and incubated with ox-LDL for additional 24 h. Then, immunofluorescence staining was performed using a monoclonal antibody against rabbit LOX-1 or a polyclonal antibody against PCNA. Ox-LDL was purchased from Biogenesis. All the experiments were performed in triplicate, and each experiment was repeated three times.

Human atherectomy specimens. To investigate the expression of LOX-1 in restenotic lesions from humans, we performed immunohistochemical analysis of atherectomy specimens after angioplasty with an anti-LOX-1 antibody as reported previously [9]. In order to further assess relationships between LOX-1 expression and the presence of ox-LDL in SMC of restenotic lesions, we performed immunohistochemical staining with a monoclonal antibody raised against ox-LDL. In addition, to address the role of LOX-1 in restenosis after PCI, colocalization of LOX-1 and PCNA was analyzed by double immunofluorescence staining, using a polyclonal antibody raised against PCNA (Santa Cruz Biotechnology).

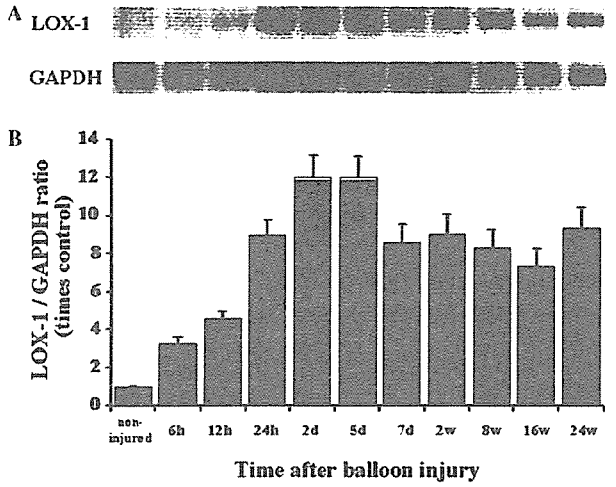

Fig. 1. Time course of LOX-1 mRNA expression after balloon injury in the rabbit aorta. Total RNA was isolated from the non-injured aorta, and the injured aorta obtained at 6 hours (6h), 12 hours (12h), 24 hours (24h), 2 days (2d), 5 days (5d), 7 days (7d), 2 weeks (2w), 8 weeks (8w), 16 weeks (16w), and 24 weeks (24w) after balloon injury. (A) A representative time course of LOX-1 mRNA expression after balloon injury by RT-PCR. (B) Quantification of LOX-1 mRNA in three independent experiments. Intensities of the bands for LOX-1 were normalized in comparison with those for GAPDH. Bars indicate fold increases relative to non-injured aorta (mean ± SD).

Statistical analysis. All calculated data are presented as means ± SD and analyzed by ANOVA. A value of $P < 0.05$ was considered to be statistically significant.

Results

Vascular injury model of the rabbit aorta

We used a balloon-injury model of rabbit aorta in which LOX-1 mRNA and protein expression levels were analyzed at 6, 12, and 24 h, 2, 5, and 7 days, and 2, 4, 8, 16, and 24 weeks after the balloon injury. Neointima appeared 5 days after balloon injury and the neointimal area increased until 8 weeks (data not shown). We have previously shown that not only media, but also the neointima, are composed predominantly of SMC based on immunohistochemical staining for muscle actin [9].

Time course of LOX-1 mRNA expression

Based on RT-PCR analysis for the time-dependent changes in LOX-1 mRNA expression after balloon injury, LOX-1 mRNA expression was minimal in the non-injured aorta, showed a peak level 2 days after the injury (a 12-fold increase compared with non-injured aorta), declined slightly from the peak value after 7 days, and remained elevated until 24 weeks after injury (Fig. 1).

Expression of LOX-1 protein

To analyze the localization of LOX-1 protein in the balloon-injured rabbit aorta, we performed immunohistochemical staining with a monoclonal antibody raised against rabbit LOX-1 (Fig. 2A). The LOX-1 protein was

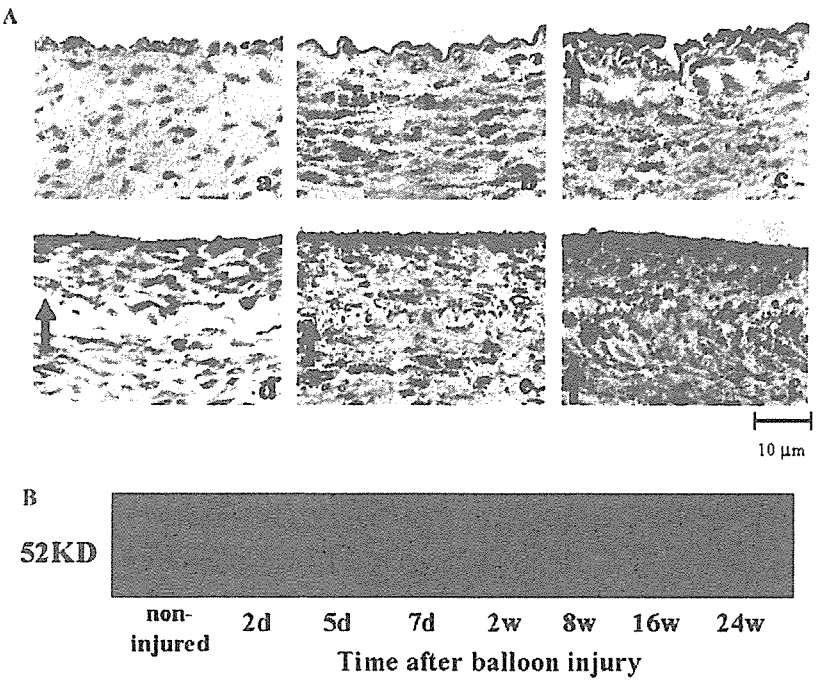

Fig. 2. Immunohistochemical staining for LOX-1 in the balloon-injured rabbit aorta. (A) Representative pictures of immunohistochemical staining. LOX-1 protein was not detected in the media of the non-injured aorta (a), but was expressed in SMC of the media at 2 days (b) after balloon injury, as well as in the SMC of the media and neointima at 5 days (c), 2 weeks (d), 8 weeks (e), and 24 weeks (f) after balloon injury. Arrows indicate the internal elastic lamina. (B) Time course of LOX-1 protein expression after balloon injury in the rabbit aorta by Western blot analysis.

not detectable in the media of non-injured aorta, but was expressed in the medial SMC 2 days after vascular injury. Five days after injury, neointimal formation was observed and LOX-1 protein was expressed in both medial and neointimal SMC. LOX-1 protein expression persisted in the medial and neointimal SMC until 24 weeks after injury.

Furthermore, in order to quantify the expression levels of LOX-1 protein after vascular injury, Western blot analysis of LOX-1 was performed. The time course of LOX-1 protein expression is shown in Fig. 2B. The expression of LOX-1 was undetectable in the non-injured aorta, but appeared at 2 days after vascular injury, gradually increased, and sustained until 24 weeks after injury.

In situ hybridization of LOX-1 mRNA

We performed *in situ* hybridization to assess whether medial and neointimal SMC produced mRNA encoding LOX-1. LOX-1 mRNA was not detected in the medial SMC of non-injured aortas, whereas LOX-1 mRNA was expressed in the medial and neointimal SMC at both 2 and 24 weeks after injury (Fig. 3), as well as in the medial SMC 2 days after injury (data not shown).

Effect of LOX-1 on SMC proliferation

In order to clarify the role of LOX-1 in neointimal formation after vascular injury, we performed cell culture experiments using cultured rabbit SMC, ox-LDL, and antisense or sense LOX-1. Using immunofluorescence staining, we analyzed the expression of LOX-1 and PCNA. Immunofluorescence staining demonstrated that ox-LDL (10 μg/mL) upregulated the expression of both LOX-1 and PCNA (Figs. 4B and F). In addition, antisense LOX-1 decreased the ox-LDL-induced expression of LOX-1 and PCNA (Figs. 4C and G); however, sense

Fig. 3. In situ hybridization of LOX-1 in the balloon-injured rabbit aorta. Using an antisense probe, LOX-1 mRNA was not detected in the media of the non-injured aorta (A), but was observed in SMC of the media and neointima at 2 (C) and 24 (E) weeks after balloon injury. Using a sense probe, no signal was detected in the non-injured aorta (B), or the aorta at 2 (D) or 24 (F) weeks after balloon injury. Arrows indicate the internal elastic lamina.

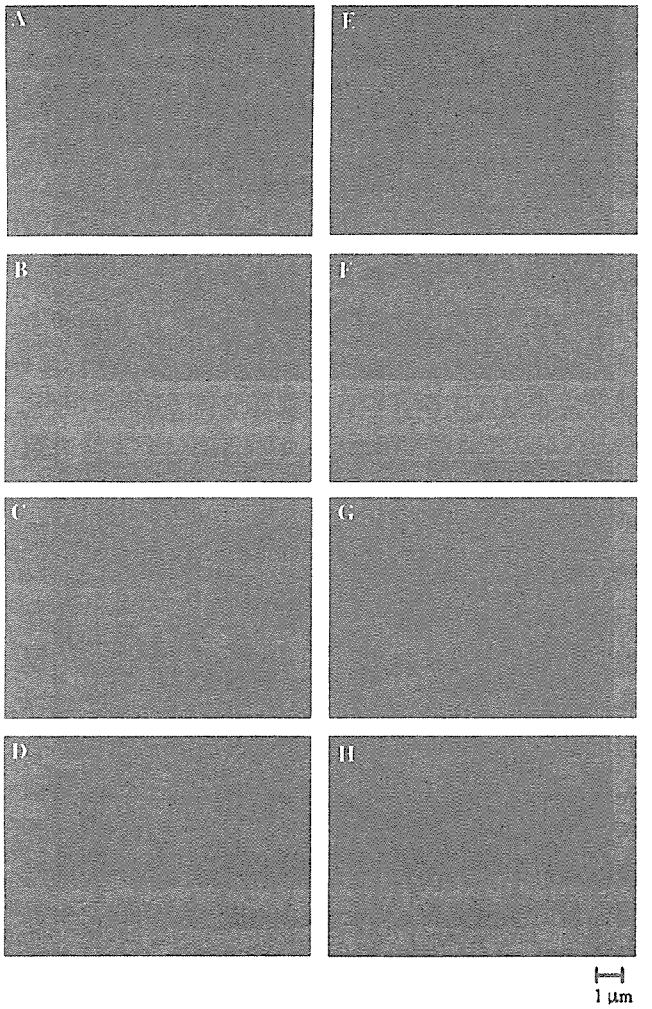

Fig. 4. Immunofluorescence staining for LOX-1 (A–D) and PCNA (E–H) in cultured SMC. (A,E) 0.1% FBS; (B,F) 0.1% FBS + 10 μg/mL ox-LDL; (C,G) 0.1% FBS + 10 μg/mL ox-LDL + antisense LOX-1; (D,H) 0.1% FBS + 10 μg/mL ox-LDL + sense LOX-1. Ox-LDL upregulated the expression of LOX-1 (B) and PCNA (F). Antisense LOX-1 decreased the ox-LDL-induced expression of LOX-1 (C) and PCNA (G); however, sense LOX-1 did not affect the ox-LDL-stimulated expression of LOX-1 (D) or PCNA (H).

LOX-1 did not affect the ox-LDL-induced LOX-1 or PCNA expression (Figs. 4D and H). Furthermore, we analyzed proliferation of SMC by counting the cell numbers of cultured SMC 3 days after stimulation by ox-LDL (Fig. 5), and found that ox-LDL (10 μg/mL) significantly increased the cell number. Preincubation of SMC with antisense LOX-1, but not sense LOX-1, significantly suppressed the ox-LDL-induced increase in the cell number.

Expression of LOX-1 in human restenotic lesion

To determine if LOX-1 was expressed in human restenotic lesions after balloon-angioplasty, we performed immunohistochemical analysis, using an anti-rabbit LOX-1 monoclonal antibody in human atherectomy specimens obtained from human coronary restenotic lesions.

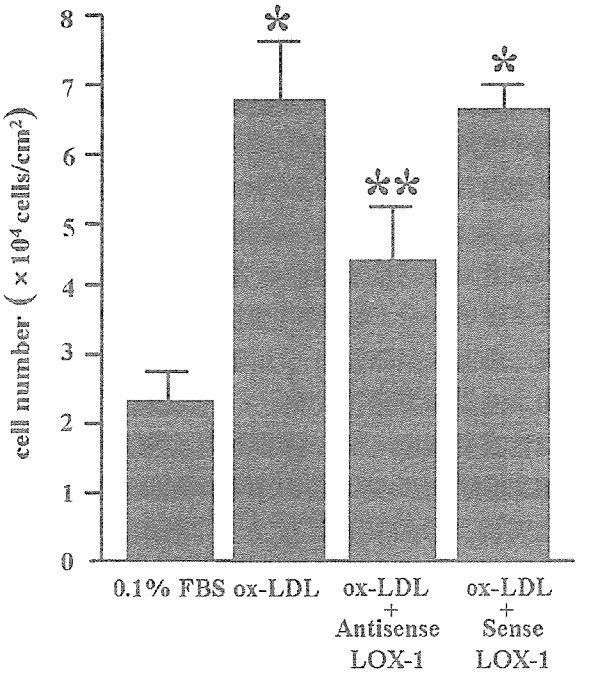

Fig. 5. Effect of antisense LOX-1 on SMC proliferation. Ox-LDL (10 μg/mL) significantly increased the number of SMC. Preincubation of SMC with antisense LOX-1, but not sense LOX-1, significantly decreased the cell number. *$P < 0.01$ vs. 0.1% FBS, **$P < 0.01$ vs. ox-LDL or ox-LDL + sense LOX-1.

LOX-1 was strongly expressed in human restenotic lesions after balloon-angioplasty (Figs. 6A and B). Oxidized LDL was also detected in the intimal SMC of human restenotic lesions, suggesting colocalization of LOX-1 and ox-LDL in human coronary restenotic lesions (Figs. 6C and D). Furthermore, double immunofluorescence staining revealed a colocalization of LOX-1 and PCNA in restenotic lesion after PCI (Figs. 6E and F). It is suggested that LOX-1 appears to be involved in SMC proliferation in restenosis after PCI.

Discussion

In this study, we demonstrated that LOX-1 mRNA and protein are induced and persistently expressed in neointimal and medial SMC of the rabbit aorta for 24 weeks after balloon injury. LOX-1 protein is similarly expressed in restenotic lesions after balloon-angioplasty in humans. In cell culture experiments, the chemical inhibitor of LOX-1 reduced the SMC proliferation stimulated by relatively low concentrations of ox-LDL which was hard to induce apoptosis, although previous studies have shown that higher concentrations induce LOX-1-dependent apoptosis of SMC [14,15]. These results suggest that LOX-1 may play a role in restenosis after PCI and that LOX-1 might be a molecular target for preventing restenosis after PCI.

LOX-1 has been reported to be upregulated by proinflammatory stimuli, such as tumor necrosis factor-alpha (TNF-α) [16,17], transforming growth factor-beta (TGF-β) [18], and

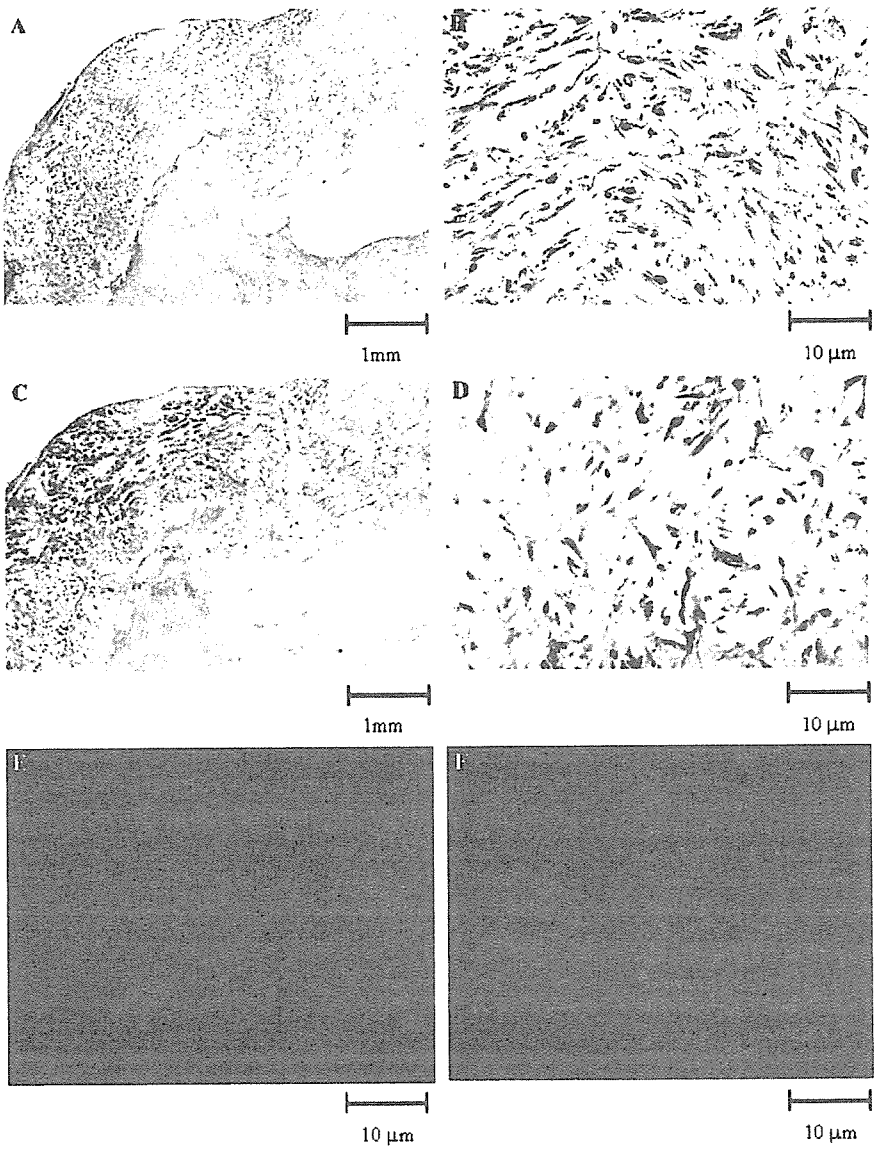

Fig. 6. Expression of LOX-1 (A,B) and oxidized LDL (C,D) in human restenotic lesions by immunohistochemistry. (A,C) Low power magnification; (B,D) high power magnification. Double immunofluorescense staining showed a colocalization of LOX-1 and PCNA in restenotic lesion after PCI (E, LOX-1; F, PCNA).

bacterial endotoxin [17], as well as by phorbol esters [16], angiotensin II [20,21], oxidized LDL [13,22], fluid shear stress [19,23], and heparin-binding epidermal growth factor-like growth factor (HB-EGF) [24]. Specifically, angiotensin II, TGF-β, and HB-EGF are known to play roles in restenosis after balloon injury or atherogenesis of human coronary arteries. Furthermore, Mehta et al. [25,26] reported that statins and aspirine inhibit ox-LDL-mediated LOX-1 expression in endothelial cells.

In the present study, we also demonstrated that LOX-1 colocalizes with ox-LDL in human restenotic lesions after balloon-angioplasty. This suggests that the interaction between ox-LDL and LOX-1 appears to occur in human coronary restenotic lesions and that ox-LDL may be one of the stimuli that induce LOX-1 expression and smooth muscle cell proliferation after balloon injury. LOX-1 also is reported to be the receptor for apoptotic cells, in addition to ox-LDL [13].

Significant numbers of apoptotic cells are present in restenotic lesions after balloon injury [27]. Higher concentrations of ox-LDL can induce smooth muscle cell apoptosis by the interactions with LOX-1 [14,15]. Moreover, LOX-1 can act as a phagocytic receptor for apoptotic cells [28]. Therefore, LOX-1 may also play an important role in inducing and removing apoptotic cells from restenotic lesions after PCI [28].

Recently, Muscali et al. [29] reported that LOX-1 was expressed in neointima of rat common carotid artery until 2 weeks after balloon injury. Here, we demonstrated that LOX-1 was induced in neointima and media of rabbit aorta

in a time-dependent manner and its expression was sustained until 24 weeks after balloon injury. Muscali et al. did not show the direct evidence that LOX-1 is associated with SMC proliferation. Therefore, we performed the cell culture experiments in order to address the role of LOX-1 in restenotic lesion after PCI. Relatively low concentrations of ox-LDL stimulated the SMC proliferation, which was inhibited by antisense LOX-1. In addition, for the first time, we demonstrated the expression of LOX-1 and its colocalization with PCNA in human restenotic lesion by double immunofluorescense staining. Our results thus suggest that LOX-1 appears to play significant roles in proliferation of SMC.

LOX-1 has been reported to be converted into soluble molecules by proteolytic cleavage at the membrane-proximal sites of the extracellular domain [30]. Among the scavenger receptors, LOX-1 is the first molecule shown to be cleaved from the cell surface and released as a soluble molecule. Recently, soluble LOX-1 was reported to be a useful marker for early diagnosis of acute coronary syndrome [31]. We speculate that the concentration of soluble LOX-1 in the circulating plasma might also be elevated in patients with restenosis after PCI, and thus might possibly be a predictor or indicator of restenosis after PCI.

In conclusion, the present study revealed that LOX-1 is expressed by SMC in the media and neointima after balloon injury in humans and animal models in a time-dependent fashion. Furthermore, immunohistostaining and cell culture experiments demonstrated that LOX-1 appears to be involved in ox-LDL-induced SMC proliferation. LOX-1 thus may play a key role in neointimal formation and restenosis after balloon-angioplasty and may be one of the target molecules for the diagnosis and prevention of restenosis after PCI.

References

[1] R. Ross, Atherosclerosis—an inflammatory disease, N. Engl. J. Med. 340 (1999) 115–126.

[2] T. Sawamura, N. Kume, T. Aoyama, H. Moriwaki, H. Hoshikawa, Y. Aiba, T. Tanaka, S. Miwa, Y. Katsura, T. Kita, T. Masaki, An endothelial receptor for oxidized low-density lipoprotein, Nature 386 (1997) 73–77.

[3] H. Kataoka, N. Kume, S. Miyamoto, M. Minami, T. Murase, T. Sawamura, T. Masaki, N. Hashimoto, T. Kita, Expression of lectin-like oxidized low-density lipoprotein receptor-1 in human atherosclerotic lesions, Circulation 99 (1999) 3110–3117.

[4] N. Kume, T. Kita, Roles of lectin-like oxidized LDL receptor-1 and its soluble forms in atherogenesis, Curr. Opin. Lipidol. 12 (2001) 419–423.

[5] K. Inoue, Y. Arai, H. Kurihara, T. Kita, T. Sawamura, Overexpression of lectin-like oxidized low-density lipoprotein receptor-1 induces intramyocardial vasculopathy in apolipoprotein E-null mice, Circ. Res. 97 (2005) 176–184.

[6] M.C. Morice, P.W. Serruys, J.E. Sousa, J. Fajadet, E. Ban Hayashi, M. Perin, A. Colombo, G. Schuler, P. Barragan, G. Guagliumi, F. Molnar, R. Falotico, RAVEL Study Group, A randomized comparison of a sirolimus-eluting stent with a standard stent for coronary revascularization, N. Engl. J. Med. 346 (2002) 1773–1780.

[7] G.W. Stone, S.G. Ellis, D.A. Cox, J. Hermiller, C. O'Shaughnessy, J.T. Mann, M. Turco, R. Caputo, P. Bergin, J. Greenberg, J.J. Popman, M.E. Russell, TAXUS-IV Investigators, A polymer-based, paclitaxel-eluting stent in patients with coronary artery disease, N. Engl. J. Med. 350 (2004) 221–231.

[8] M.N. Babapulle, L. Joseph, P. Belisle, J.M. Brophy, M.J. Eisenberg, A hierarchical Bayesian meta-analysis of randomised clinical trials of drug-eluting stents, Lancet 364 (2004) 583–591.

[9] M. Miyata, S. Biro, H. Kaieda, H. Eto, K. Orihara, T. Kihara, H. Obata, N. Matsushita, T. Matsuyama, C. Tei, Apolipoprotein J/Clusterin is induced in vascular smooth muscle cells after vascular injury, Circulation 104 (2001) 1407–1412.

[10] H. Eto, S. Biro, M. Miyata, H. Kaieda, H. Obata, T. Kihara, K. Orihara, C. Tei, Angiotensin II type 1 receptor participates in extracellular matrix production in the late stage of remodeling after vascular injury, Cardiovasc. Res. 59 (2003) 200–211.

[11] K. Orihara, S. Biro, S. Hamasaki, H. Eto, M. Miyata, Y. Ikeda, C. Tei, Hyperthermia at 43 °C for 2 h inhibits the proliferation of vascular smooth muscle cells, but not endothelial cells, J. Mol. Cell. Cardiol. 34 (2002) 1205–1215.

[12] D. Li, J.L. Mehta, Antisense to LOX-1 inhibits oxidized LDL-mediated upregultaion of monocyte chemoattractant protein-1 and monocyte adhesion to human coronary artery endothelial cells, Circulation 101 (2000) 2889–2895.

[13] D. Li, J.L. Mehta, Upregulation of endothelial receptor for oxidized LDL (LOX-1) by oxidized LDL and implications in apoptosis of human coronary artery endothelial cells: evidence from use of antisense LOX-1 mRNA and chemical inhibitors, Arterioscler. Thromb. Vasc. Biol. 20 (2000) 1116–1122.

[14] K. Kataoka, K. Hasegawa, T. Sawamura, M. Fujita, T. Yanazume, E. Iwai-Kanai, T. Kawamura, T. Hirai, T. Kita, R. Nohara, LOX-1 pathway affects the extent of myocardial ischemia–reperfusion injury, Biochem. Biophys. Res. Commun. 300 (2003) 656–660.

[15] N. Kume, T. Kita, Apoptosis of vascular cells by oxidized LDL: Involvement of caspase and LOX-1 and its implication in atherosclerotic plaque rupture, Circ. Res. 94 (2004) 269–270.

[16] N. Kume, T. Murase, H. Moriwaki, T. Aoyama, T. Sawamura, T. Masaki, T. Kita, Inducible expression of lectin-like oxidized low density lipoprotein receptor-1 in vascular endothelial cells, Circ. Res. 83 (1998) 322–327.

[17] H. Moriwaki, N. Kume, H. Kataoka, T. Murase, E. Nishi, T. Sawamura, T. Masaki, T. Kita, Expression of lectin-like oxidized low density lipoprotein receptor-1 in human and murine macrophages: upregulated expression by TNF-alpha, FEBS Lett. 440 (1998) 29–32.

[18] M. Minami, N. Kume, H. Kataoka, M. Morimoto, K. Hayashida, T. Sawamura, T. Masaki, T. Kita, Transforming growth factor-beta 1 increased the expression lectin-like oxidized low density lipoprotein receptor-1, Biochem. Biophys. Res. Commun. 272 (2000) 357–361.

[19] M. Nagase, J. Abe, K. Takahashi, J. Ando, S. Hirose, T. Fujita, Genomic organization and regulation of expression of the lectin-like oxidized low-density lipoprotein receptor (LOX-1) gene, J. Biol. Chem. 273 (1998) 33702–33707.

[20] H. Morawietz, U. Rueckscholoss, B. Niemann, N. Duerrschmidt, J. Galle, K. Hakim, H.R. Zerkowski, T. Sawamura, J. Holtz, Angioteinsin II induces LOX-1, the human endothelial receptor for oxidized low-density lipoprotein, Circulation 100 (1999) 899–902.

[21] D.Y. Li, Y.C. Zhang, M.I. Philips, T. Sawamura, J.L. Mehta, Upregulation of endothelial receptor for oxidized low-density lipoprotein (LOX-1) in cultured human coronary artery endothelial cells by angiotensin II type 1 receptor activation, Circ. Res. 84 (1999) 1043–1049.

[22] T. Aoyama, H. Fujiwara, T. Masaki, T. Sawamura, Induction of lectin-like oxidized LDL receptor by oxidized LDL and lysophosphatidylcholine in cultured endothelial cells, J. Mol. Cell. Cardiol. 31 (1999) 2101–2114.

[23] T. Murase, N. Kume, R. Korenaga, J. Ando, T. Sawamura, T. Masaki, T. Kita, Fluid shear stress transcriptionally induces lectin-like oxidized low density lipoprotein receptor-1 in vascular endothelial cells, Circ. Res. 83 (1998) 328–333.

[24] E. Mukai, N. Kume, K. Hayashida, M. Minami, Y. Yamada, Y. Seino, T. Kita, Heparin-binding EGF-like growth factor induces expression of lectin-like oxidized LDL receptor-1 in vascular smooth muscle cells, Atherosclerosis 176 (2004) 289–296.
[25] D.Y. Li, H.J. Chen, J.L. Mehta, Statins inhibit oxidized-LDL-mediated LOX-1 expression, uptake of oxidized-LDL and reduction in PKB phosphorylation, Cardiovasc. Res. 52 (2001) 130–135.
[26] J.L. Mehta, J. Chen, F. Yu, D.Y. Li, Aspirin inhibits ox-LDL-mediated LOX-1 expression and metalloproteinase-1 in human coronary endothelial cells, Cardiovasc. Res. 64 (2004) 243–249.
[27] J.M. Isner, M. Kearney, S. Bortmann, J. Passeri, Apoptosis in human atherosclerosis and restenosis, Circulation 91 (1995) 2703–2711.
[28] K. Oka, T. Sawamura, K. Kikuta, S. Itokawa, N. Kume, T. Kita, T. Masaki, Lectin-like oxidized low-density lipoprotein receptor 1 mediates phagocytosis of aged/apoptotic cells in endothelial cells, Proc. Natl. Acad. Sci. USA 95 (1998) 9535–9540.
[29] C. Muscoli, I. Sacco, W. Alecce, E. Palma, R. Nistico, N. Costa, F. Clementi, D. Rotiroti, F. Romeo, D. Salvemini, J.L. Mehta, V. Mollace, The protective effect of superoxide dismutase mimetic M40401 on balloon injury-related neointima formation: role of the lectin-like oxidized low-density lipoprotein receptor-1, J. Phamacol. Exp. Ther. 311 (2004) 44–50.
[30] T. Murase, N. Kume, H. Kataoka, M. Minami, T. Sawamura, T. Masaki, T. Kita, Identification of soluble forms of lectin-like oxidized LDL receptor-1, Arterioscler. Thromb. Vasc. Biol. 20 (2000) 715–720.
[31] K. Hayashida, N. Kume, T. Murase, M. Minami, D. Nakagawa, T. Inada, M. Tanaka, A. Ueda, G. Kominami, H. Kambara, T. Kimura, T. Kita, Serum soluble lectin-like oxidized low-density lipoprotein receptor-1 levels are elevated in acute coronary syndrome: a novel marker for early diagnosis, Circulation 112 (2005) 812–818.

Histone Acetyltransferase Activity of p300 Is Required for the Promotion of Left Ventricular Remodeling After Myocardial Infarction in Adult Mice In Vivo

Shoichi Miyamoto, MD*; Teruhisa Kawamura, MD, PhD*; Tatsuya Morimoto, MD, PhD; Koh Ono, MD, PhD; Hiromichi Wada, MD, PhD; Yosuke Kawase, PhD; Akira Matsumori, MD, PhD; Ryosuke Nishio, MD, PhD; Toru Kita, MD, PhD; Koji Hasegawa, MD, PhD

Background—Left ventricular (LV) remodeling after myocardial infarction is associated with hypertrophy of surviving myocytes and represents a major process that leads to heart failure. One of the intrinsic histone acetyltransferases, p300, serves as a coactivator of hypertrophy-responsive transcriptional factors such as a cardiac zinc finger protein GATA-4 and is involved in its hypertrophic stimulus-induced acetylation and DNA binding. However, the role of p300-histone acetyltransferase activity in LV remodeling after myocardial infarction in vivo is unknown.

Methods and Results—To solve this problem, we have generated transgenic mice overexpressing intact p300 or mutant p300 in the heart. As the result of its 2–amino acid substitution in the p300-histone acetyltransferase domain, this mutant lost its histone acetyltransferase activity and was unable to activate GATA-4–dependent transcription. The two kinds of transgenic mice and the wild-type mice were subjected to myocardial infarction or sham operation at the age of 12 weeks. Intact p300 transgenic mice showed significantly more progressive LV dilation and diminished systolic function after myocardial infarction than wild-type mice, whereas mutant p300 transgenic mice did not show this.

Conclusions—These findings demonstrate that cardiac overexpression of p300 promotes LV remodeling after myocardial infarction in adult mice in vivo and that histone acetyltransferase activity of p300 is required for these processes. **(*Circulation*. 2006;113:679-690.)**

Key Words: hypertrophy ■ myocytes ■ signal transduction

Left ventricular (LV) remodeling after myocardial infarction (MI) consists of dynamic changes in ventricular heart. It has been reported that among patients with acute MI, 20% had heart failure at the time of hospital admission and 9% have development of heart failure thereafter.[1] The hospital death rates associated with heart failure are greater in the latter. Therefore, elucidating the mechanisms of LV remodeling after MI is of clinical importance. During LV remodeling, hypertrophy of each surviving myocyte occurs in proportion to infarct size.[2]

Clinical Perspective p 690

Hypertrophic stimuli initiate a number of subcellular signaling pathways, which finally reach the nuclei of cardiac myocytes and change the pattern of gene expression.[3,4] Transcription factors that mediate these changes include myocyte enhancing factor-2,[5] serum response factor,[6] AP-1,[7] and a zinc finger protein, GATA-4.[7,8] The involvement of multiple transcription factors in hypertrophic responses suggests that these factors are coordinately activated.

An adenovirus E1A-associated protein, p300, acts as a coactivator of these hypertrophy-responsive transcription factors. In addition, p300 serves as an intrinsic histone acetyltransferase (HAT) and promotes an active chromatin configuration.[9–11] p300 protein can also acetylate certain nonhistone proteins such as DNA-binding transcription factors.[11–14] Acetylation is emerging as a posttranslational modification that is essential for the regulation of transcription and that modifies transcription factor affinity for binding sites on DNA, stability, and/or nuclear localization. Our previous study demonstrated that p300 can induce the acetylation and DNA binding of GATA-4. During myocardial cell hypertrophy, the acetylated form of GATA-4 and its DNA binding markedly increase, concomitant with an increase in p300 expression. In addition, a dominant-negative form of p300 inhibits agonist-induced

Received April 20, 2005; de novo received August 26, 2005; revision received October 17, 2005; accepted November 22, 2005.

From the Department of Cardiovascular Medicine, Graduate School of Medicine, Kyoto University, Kyoto, Japan (S.M., T.M., A.M., R.N., T. Kita); the Division of Translational Research, Kyoto Medical Center, National Hospital Organization, Kyoto, Japan (T. Kawamura, K.O., H.W., K.H.); and the Chugai Research Institute for Medical Science, Inc, Pharmacology & Pathology Research Center, Shizuoka, Japan (Y.K.).

*Drs Miyamoto and Kawamura contributed equally to this work.

Correspondence to Dr Koji Hasegawa, Division of Translational Research, Kyoto Medical Center, National Hospital Organization, 1-1 Mukaihata-cho, Fukakusa, Fushimi-ku, Kyoto, 612-8555, Japan. E-mail koj@kuhp.kyoto-u.ac.jp

Circulation is available at http://www.circulationaha.org

DOI: 10.1161/CIRCULATIONAHA.105.585182

hypertrophy, demonstrating a critical role of p300 in hypertrophic responses in cardiac myocytes in culture.[15] However, the precise role of p300 HAT activity in LV remodeling after MI in vivo is unknown. The present study was performed to solve this problem.

Methods

Plasmid Constructs

The expression vectors pcDNAG4, pCMVβ-gal, pCMVwtp300, and pCMVHATmutp300 contain the cytomegalovirus promoter/enhancer fused to cDNA encoding murine GATA-4,[16,17] β-galactosidase, a full-length human intact p300, or mutant p300, in which double amino acid substitution mutations were introduced,[18,19] respectively. pCMVwtp300 and pCMVHATmutp300 were gifts from Dr Richard Eckner, University of Medicine and Dentistry of NJ. The reporter plasmid pANF-luc consists of the firefly luciferase (luc) cDNA driven by a 131-bp rat atrial natriuretic factor (ANF) promoter sequence.[20] pET-1-CAT contains the transcription start site-proximal 204 bp of the wild-type (WT) rat endothelin-1 (ET-1) promoter fused to a bacterial chloramphenicol acetyltransferase (CAT) gene.[15] pRSVCAT and pRSVluc contain a bacterial CAT and a firefly luc gene, respectively, driven by Rous sarcoma virus (RSV) long terminal repeat sequences.[8]

Analysis of the Acetylation State of GATA-4 and Western Blotting

Cell culture of COS7 cells, immunoprecipitation, and Western blotting for acetylated lysine and GATA-4 were performed as previously described.[15] We used goat anti–GATA-4 polyclonal antibody (Santa Cruz Biotechnology) for immunoprecipitation, and rabbit polyclonal antibody against acetylated lysine (Cell Signaling), rabbit anti–GATA-4 polyclonal antibody (Santa Cruz Biotechnology), mouse anti-p300 monoclonal antibody (Upstate Biotechnology), mouse anti–β-actin monoclonal antibody (SIGMA), and mouse anti-GAPDH monoclonal antibody (Molecular Probes) for Western blotting. The level of acetylated GATA-4 was also analyzed by pulse-labeling as previously described.[15]

Electrophoretic Mobility Shift Assays

Electrophoretic mobility shift assays (EMSAs), with the GATA-4 site in the rat ET-1 promoter used as a probe, were carried out as previously described.[20] We also used a double-stranded oligonucleotide containing the Sp-1 binding site as a control probe (Santa Cruz Biotechnology).

Transfection and Luciferase/CAT Assays

COS7 cells were transfected with the indicated amounts of plasmid DNA through the use of LIPOFECTAMINE (Life Technologies, Inc), as previously described.[20] The relative luc or CAT activities in the same cell lysates were measured as described previously.[20]

Creation of Transgenic Mice

All animal experimental protocols were approved by the Institute of Laboratory Animals, Graduate School of Medicine, Kyoto University. Transgenic (Tg) mice overexpressing HATmut p300 (HATmut p300-Tg mice) in the heart were created as previously described.[15] Briefly, the α-myosin heavy chain (MHC)-HATmutp300 DNA plasmid was constructed by subcloning the *NotI-HindIII* fragment of pCMVHATmutp300 into the *SalI-HindIII* site of a 5.5-kb mouse α-MHC promoter–containing construct. The α-MHC-HATmutp300 DNA fragment was gel-purified and injected into newly fertilized C57BL/6 oocytes, which were transferred to the oviducts of pseudopregnant C57BL/6 recipients. All animals were maintained under specific pathogen-free conditions.

Experimental MI and Physiological Studies

All mice used in the present study were female. Mice were anesthetized with 1.0 to 1.5% isoflurane, and open-chest coronary artery ligation was performed. MI was induced by ligating the left anterior descending coronary artery. In sham-operated mice, the suture was passed but not tied. Five weeks after the operation, we noninvasively measured heart rate and blood pressure with a photoelectric pulse device (UR-5000, Ueda Production Corp) placed on the tail of prewarmed mice. We then performed echocardiography under anesthesia with 2.5% avertin. Transthoracic echocardiography was performed with a cardiac ultrasound recorder (Philips Sonos 5500), using a 12-MHz transducer. For cardiac catheterization, mice were anesthetized with a mixture of ketamine (100 mg/kg) and xylazine (5 mg/kg) intraperitoneally. The pressure-volume loops and intracardiac ECG were monitored online, and the conductance, pressure, and intracardiac electrocardiographic signals were digitized at 2 kHz, stored on disk, and analyzed as previously described.[21]

Histological Analysis

After the physiological analysis, all surviving mice were euthanized, and their hearts were removed. The excised hearts were cut into 2 transverse slices at the mid level of the papillary muscles: the basal specimens were fixed in 10% buffered formalin and embedded in paraffin, after which 4-μm-thick sections were stained with hematoxylin and eosin, Masson trichrome, and sirius red CI 35870 (0.05% solution in saturated aqueous picric acid). Quantitative assessments of infarct size, noninfarct size, cross-sectional myocardial cell diameter, cell populations, and fibrotic area were performed on 20 randomly chosen high-power fields in each section with the use of Axioskop 2 FS plus (Zeiss).

Measurement of Myocardial ET-1 Levels

ET-1 was extracted from the supernatant of homogenized LV tissues and measured by means of the sandwich enzyme immunoassay, as previously described.[22]

Statistical Analysis

Data are presented as mean±SD. Statistical comparisons were performed with the use of unpaired 2-tailed Student *t* tests or ANOVA with Scheffé test where appropriate, with a probability value <0.05 taken to indicate significance. The log-rank test was used to evaluate survival rate.

Results

HAT Activity of p300 Is Required for Acetylation and DNA Binding of GATA-4

To determine the role of p300 HAT activity in acetylation and DNA binding of GATA-4, we performed experiments using pCMVHATmutp300, an expression plasmid encoding mutant p300 (HATmut p300). We performed immunoprecipitation/Western blotting in COS7 cells transfected with pcDNAG4 in the presence or absence of pCMVwtp300 or pCMVHATmutp300. No protein was immunoprecipitated with control IgG (Figure 1A, lane 4). Forced expression of intact p300 induced acetylation of GATA-4, whereas expression of HATmut p300 did not induce acetylation (Figure 1A, upper panel). GATA-4 was similarly immunoprecipitated with anti–GATA-4 antibody in the 3 groups (Figure 1A, lower panel). Before immunoprecipitation, the expression levels of GATA-4 were similar in the 3 groups (Figure 1B, middle panel). Furthermore, intact p300 and HATmut p300 were expressed at similar levels (Figure 1B, upper panel). We also performed pulse-labeling experiments. Incorporation of sodium [^{14}C]acetate into GATA-4 protein was clearly detected in pCMVwtp300-transfected cells but not in pCMVHATmutp300-

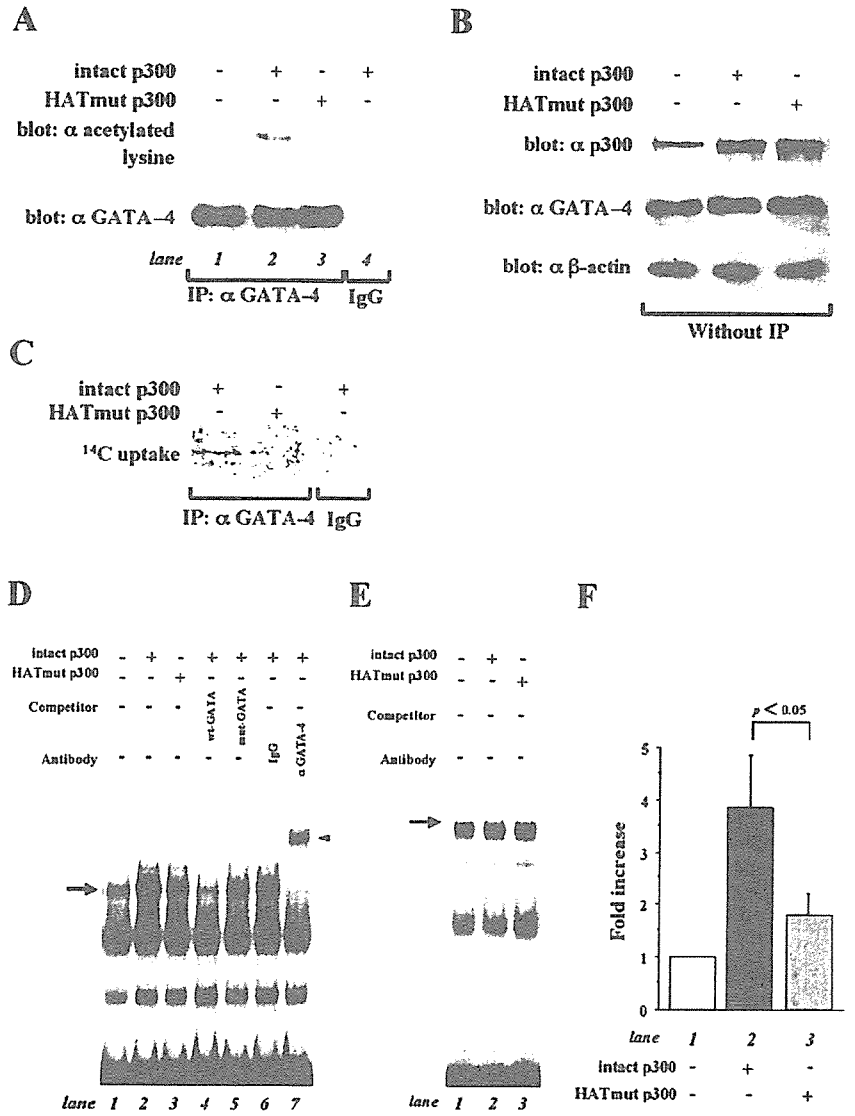

Figure 1. Histone acetyltransferase (HAT) activity of p300 is required for acetylation and DNA binding of GATA-4. A, COS7 cells were transfected with 2 μg of pcDNAG4 in the presence or the absence of pCMVwtp300 (10 μg) or pCMVmutp300 (10 μg), as indicated. The total amount of DNA was kept constant by cotransfecting pCMVβ-gal. Protein extracts from these cells were immunoprecipitated with goat anti-GATA-4 polyclonal antibody, followed by sequential Western blotting with rabbit antiacetylated lysine polyclonal antibody and with rabbit anti-GATA-4 polyclonal antibody. B, The extracts used in A before immunoprecipitation were subjected to Western blotting with the use of antibodies against p300, GATA-4, and β-actin. C, COS7 cells were transfected with 2 μg of pcDNAG4 in addition to 10 μg of pCMVwtp300 or pCMVmutp300 and were pulse-labeled with [14C] acetic acid, sodium salt for 3 hours. The protein extracts were immunoprecipitated with goat anti-GATA-4 polyclonal antibody or with normal goat IgG and resolved by SDS-PAGE. D and E, The same extracts used in A and B were probed with a radiolabeled double-stranded oligonucleotide containing the GATA-4 site in the ET-1 promoter (D) and with one containing the Sp-1 site (E). F, The amount of GATA-4/DNA binding (indicated by an arrow) was quantified by densitometry with the use of NIH image 1.61.

transfected ones (Figure 1C). Next, the same extracts used in the experiments shown in Figure 1, A and B, were subjected to EMSAs by using the GATA-4 site of ET-1 promoter as a probe (Figure 1D). Competition and supershift experiments demonstrated that the retarded band (indicated by an arrow) represents an interaction of the probe with GATA-4. Notably, expression of intact p300 markedly increased GATA-4/DNA binding (lane 2) compared with β-gal expression (lane 1), whereas that of mutant p300 only modestly increased (lane 3, Figure 1, D and F). Sp-1/DNA binding was similar among the 3 groups (Figure 1E). These findings demonstrate that the HAT activity of p300 plays a critical role in acetylation and DNA binding of GATA-4.

HAT Activity of p300 Is Required for Synergistic Activation of GATA-4–Dependent Promoters

To examine whether the HAT activity of p300 participates in GATA-4–dependent transcription of the ET-1 and ANF genes, we performed transient transfection experiments. As shown in Figure 2, A and B, transfection of either pcDNAG4 (lane 2), pCMVwtp300 (lane 3), or pCMVHATmutp300 (lane 5) alone resulted in only modest increases in ANF and ET-1 promoter activities. Transfection of pCMVwtp300 in addition to pGATA-4 (lane 4) induced a marked activation of these promoter activities. However, transfection of pCMVHATmutp300 only modestly augmented GATA-4–dependent ET-1 or ANF transcription (lane 6). Intact p300 and HATmutant p300 were similarly expressed in extracts from pCMVwtp300-transfected and pCMVHATmutp300-transfected cells (Figure 2C, upper panel, lanes 3 to 6). GATA-4 levels were also similar among lanes 2, 4, and 6 (Figure 2C, middle panel). These findings demonstrate that p300 and GATA-4 synergistically activate the ANF and ET-1 promoters and that the HAT activity of p300 is required for these activations.

HAT Activity of p300 Is Required for Acetylation of GATA-4 in the Mouse Heart

To further investigate the role of p300 HAT activity in LV remodeling after MI in vivo, we generated Tg mice

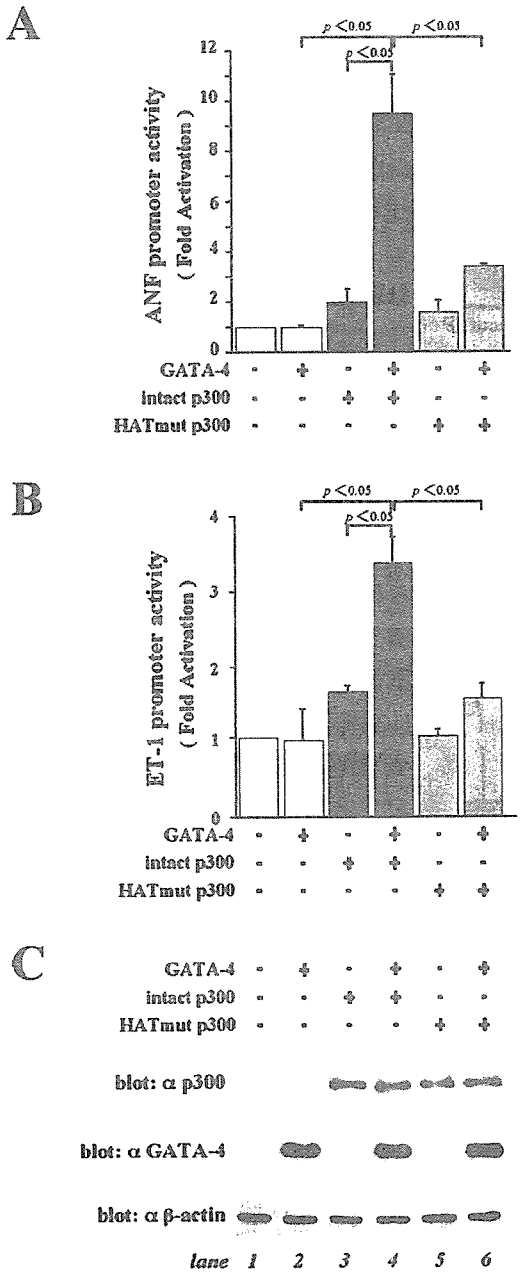

Figure 2. Histone acetyltransferase (HAT) activity of p300 participates in GATA-4–dependent activation of atrial natriuretic factor (ANF) and endothelin-1 (ET-1) promoters. A and B, COS7 cells were transfected with 2.0 μg of pANF-luc and 0.1 μg of pRSV-CAT (A) or 2.0 μg of pET-1-CAT and 0.1 μg of pRSV-luc (B) in the presence or absence of 0.5 μg of pcDNAG4 and 2.5 μg of pCMVwtp300 or pCMVmutp300, as indicated. The total amount of DNA was kept constant by cotransfecting pCMVβ-gal. The results, expressed as fold induction of reporter constructs, are mean±SD of 3 independent experiments, each carried out in duplicate. C, Extracts from these cells were subjected to Western blotting for p300, GATA-4, and β-actin.

overexpressing intact p300 or HATmut p300 in the heart. Among multiple lines we obtained, we selected two independent lines for each type of Tg mouse (intact p300-Tg: lines 21 and 39; HATmut p300-Tg: lines 17 and 23) because the expression levels of the transgene in the heart were similar among these four lines. Since similar findings were obtained for the two lines in each kind of Tg mice, we show in the present study combined data of these two lines.

At the age of 12 weeks, cardiac function and morphology of each type of Tg mice were similar to those of the corresponding WT mice. These mice were then subjected to either sham operation or MI operation. Five weeks later, extracts from the whole LV except for the scar area of these mice were subjected to Western blotting with anti-p300 antibody that recognized the proteins produced from both transgenes (intact p300 and HATmut p300) as well as endogenous p300 (Figure 3A, upper panel, and Figure 3B). In the sham operation groups, intact p300- and HATmut p300-Tg mouse hearts showed an 8-fold increase in total p300 content, compared with their corresponding WT mouse hearts (compare lanes 1 and 3 and lanes 5 and 7 in Figure 3B). Endogenous p300 levels in WT mouse hearts increased after MI (compare lanes 1 and 2 and lanes 5 and 6 in Figure 3B). However, in the hearts of intact p300-Tg and HATmut p300-Tg mice, total p300 levels were similar between the sham operation and MI groups (compare lanes 3 and 4 and lanes 7 and 8 in Figure 3B). On the other hand, the total amounts of cardiac GATA-4 were similar in all groups (Figure 3A, middle panel).

Next, we investigated the role of p300 HAT activity in GATA-4 acetylation in mouse hearts. Signals of acetylated GATA-4 (Figure 3C, upper panel) were distinct in intact p300-Tg mice (lanes 3 and 4) but undetectable or very weak in WT mice (lanes 1 and 2) and HATmut p300-Tg mice (lanes 5 and 6). In all kinds of mice, the signals were higher in the MI groups than in the sham-operated groups. GATA-4 was similarly immunoprecipitated with anti–GATA-4 antibody in all these groups (Figure 3C, lower panels, lanes 1 to 6). No protein was immunoprecipitated with control IgG (lanes 7 and 8). These findings demonstrate that the overexpression of p300 in the heart promotes the acetylation of GATA-4 and that the HAT activity of p300 is required for this effect.

Cardiac Overexpression of Intact p300 but Not of Mutant p300 Augments LV Remodeling After MI

All sham-operated mice survived throughout the study. We next examined the mortality of MI-operated mice after the operation. Mortality at day 0, which indicates acute surgical death due to MI, did not differ among WT, intact p300-Tg, and HATmut p300-Tg mice (Figure 4A). The 5-week survival rate was significantly lower in intact p300-Tg mice than the corresponding WT mice but was similar between HATmut p300-Tg and WT mice. Autopsy revealed considerable pleural effusion and pulmonary congestion in almost all of the mice that died later than 2 days after MI, suggesting that these mice predominantly died of heart failure. Compared with HATmut p300-Tg mice, the mortality rate of intact p300-Tg mice was remarkably increased later than 2 days after MI. Thus, this increase may come from increased incidence of heart failure in intact p300-Tg mice after MI.

Next, we performed physiological study to evaluate cardiac morphological and functional changes at 5 weeks

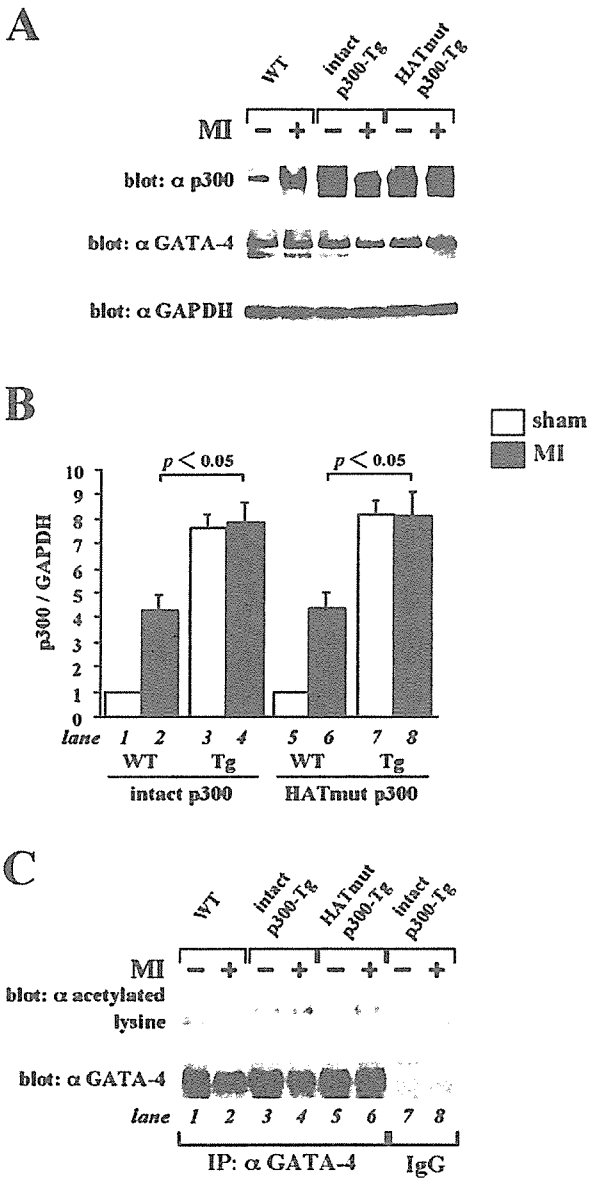

Figure 3. Histone acetyltransferase (HAT) activity of p300 is required for acetylation of GATA-4 in adult mouse hearts. A and B, Five weeks after the sham or MI operation, 10 μg of protein extracts from WT and intact p300- or HATmut p300-Tg mouse hearts were subjected to Western blotting with anti-p300 antibody, anti-GATA-4 antibody, or anti-GAPDH antibody. Representative photographs in each group are shown (A). The levels of signals were quantified, and results from 6 animals in each group are expressed as mean±SD (B). C, Protein extracts from WT and intact p300- or HATmut p300-Tg mouse hearts were immunoprecipitated with goat anti-GATA-4 polyclonal antibody or control goat IgG and sequentially subjected to Western blotting for acetylated lysine and GATA-4.

after sham or MI operation. Echocardiographic data in the sham-operation groups was similar among all kinds of mice (WT, intact p300-Tg, and HATmut p300-Tg). After MI, however, increase in LV end-diastolic and end-systolic dimension and decrease in percent fractional shortening were more prominent in intact p300-Tg than WT mice but were similar between WT and HATmut p300-Tg mice (Figure 4, B and C). Systolic and diastolic blood pressures were similar among these kinds of mice. Cardiac catheterization data (Figure 5) in the sham operation groups were also similar among all kinds of mice except for LV end-diastolic pressure, LV end-systolic volume, and τ, the time constant of isovolumic relaxation, which were slightly increased in intact p300-Tg mice. After MI, the increases in LV end-diastolic volume (LVEDV), LV end-systolic volume, and LV end-diastolic pressure and the decreases in normalized end-systolic volume elastance (NL Ees) and preload recruitable volume work were more prominent in intact p300-Tg than their corresponding WT mice but were similar between HATmut p300-Tg and their WT mice. In summary, diastolic function is impaired in intact p300-Tg mice compared with other kinds of mice. In addition, in accord with the data obtained by echocardiography, MI-induced changes, consisting of decreased contractility, chamber dilation, and low output, were more prominent in intact p300-Tg mice than in HATmut p300-Tg or WT mice.

Consistent with the findings of the physiological analysis, histological analysis at 5 weeks after MI revealed a severely dilated LV cavity with a thin infarct wall in intact p300-Tg mice compared with HATmut p300-Tg or WT mice (Figure 6A). The absolute infarct size was similar among the different kinds of mice, whereas the noninfarct area was modestly increased in intact p300-Tg mice (Figure 6B). There was no significant difference in percentages of infarct area relative to total LV area among WT (23.4%), intact p300-Tg (21.3%), and HATmut p300-Tg (22.1%) mice, suggesting that severe LV remodeling in intact p300-Tg mice developed independent of infarct size in these mice. In addition, in the MI groups, LV cavity area (Figure 6C) and heart weight/body weight ratio (Figure 6D) after MI were larger in intact p300-Tg than HATmur p300-Tg or WT mice.

Although there were no significant differences in histology among the different kinds of sham-operated mice, cross-sectional myocardial cell diameter at 5 weeks after MI was larger in intact p300-Tg mice than in WT or HATmut p300-Tg mice (Figure 7, A and B). In the MI groups, the population of noncardiomyocytes in the infarct area (Figure 7C) and the amount of fibrosis in the infarct area (Figure 7D) and in the noninfarcted LV walls (Figure 7E) were similar among WT, intact p300-Tg, and HATmut p300-Tg mice. These findings demonstrate that p300 promotes MI-induced LV remodeling associated with the hypertrophy of individual myocytes and that the HAT activity of p300 is required for this promotion.

HAT Activity of Cardiac p300 Is Involved in Increase in GATA-4/DNA binding and LV ET-1 Expression After MI

To examine changes in GATA-4/DNA-binding after MI in WT, intact p300-Tg, and HATmut p300-Tg mouse hearts, EMSAs using the ET-1 GATA site as a probe were performed in cardiac nuclear extracts from these mice 5 weeks after the operation. Competition and supershift experiments demonstrated that the retarded band (indicated by an arrow) represents an interaction of the probe with cardiac GATA-4